



UNIVERSITY OF AGDER

CONDITION BASED MAINTAINANCE FOR ROTATING MACHINERY

By

Hussein A. Mashat

**Thesis submitted in Partial Fulfillment of the
Requirements for the Degree Master of Science in
Mechatronics**

**Faculty of Engineering and Science
University of Agder**

**Grimstad
May 2010**

Statement of Originality

26th may 2010

The Head
School of Machine Engineering, Mechatronic team

The University of Agder
Groosveien 36
4876 Grimstad
Norway

In accordance with the Master of Engineering in the Faculty of Engineering (Department of Mechatronic Engineering), I hereby submit the following thesis:

“CONDITION BASED MAINTAINANCE FOR ROTATING MACHINERY”

This thesis was carried out under the supervision of Professor Kjell G. Robbersmyr and associate professor Morten K. Ebbesen.

I declare that this thesis is my original work and has not been submitted previously at the University of Agder or any other tertiary institution.

Appropriate citations are made where the content has been previously developed and is not the author's original content.

Yours sincerely

Hussein Mashat

Acknowledgements

This project would not have been possible without the help and support of all involved.

Thanks must first go to professor. Kjell G. Robbersmyr and associate professor Morten K. Ebbesen, whose supervision and guidance has led me to the successful conclusion of a project I once thought beyond me. Their assistance has been vital as both a facilitator and moderator throughout the project.

I would like to thank the other professors and lecturers in the department like Professor Michael R. Hansen, Mr. Morten Ottestad (Senior Lecturer) and the rest. mechanical workshop staff Mr. Eivind A. Johansen, Mr. Torstein K. Wroldsen and Roy W. Folgerø for their technical knowledge and support throughout the project.

Throughout my project, my friends and family have provided both support and distraction wherever necessary and I thank them for that. Thanks to the help and many timely interventions given willingly by friends, this project has led to my improving in both aspects of a successful professional Engineer, advanced technical knowledge.

Special thanks must go to my wife Zineh, who was always there to keep my ego and temper in check. Without you to keep me focused, I would never have reached where I am today. Thank you.

Master-project spring 2010

Student: Mashat Hussein

Condition Based Maintenance for Rotating Machinery

Within the offshore oil business condition based maintenance (CBM) is expected to be important in the future as large expenses are related to failure of for example rotating machinery. Therefore it is relevant to investigate this kind of systems with respect to:

- Plan maintenance together with other maintenance work on the machinery to reduce the downtime
- Increase the reliability of the machinery
- To reduce the overall cost of the offshore operation

A test rig is to be built for the purpose of testing rotating equipment. A primary concern in the design process should be an easy operation of the rig and a simple handling of the data obtained during test. The project is a continuation of the work done by the candidate in the mini-project in the autumn 2009.

The project is expected to consist of:

- Introduction (description of the objective of the project, and summary of the mini-project)
- Development of the chosen concept with respect to:
 - Structural system
 - Instrumentation, control, and data logging
 - Technical drawings, and test procedures
 - Building the rig
 - Completion of tests on the rig
- Establishing maintenance strategies based on the measurements:
 - Visual inspection and evaluation
 - Statistically and mathematically evaluation

Expenses related to the project must approved by the supervisors to be covered.

Delivering of the project is to be done in accordance with the guidelines published in the Fronter room for MAS500.

The project is carried out for:

The University of Agder, Master education in Mechatronics

Supervisors:

Kjell G. Robbersmyr phone +47 3725 3207, email kjell.g.robbersmyr@uia.no

Morten K. Ebbesen phone +47 3725 3279, email morten.k.ebbesen@uia.no

Abstract

This thesis report presents the results of a design and mathematical calculation of a mechanical test facility using SolidWorks simulation program to fine the FEM analysis of the transducer (part of the measurement device). A simplified shaft's dynamic model was investigated using SimulationX program. The purpose of this, is to develop the knowledge about the rotating shaft and the reaction forces at the boundary condition.

In this thesis, the CBM strategy is based on the model free technique and a continuous monitoring of the component(s) during the operation time. An automatic Switch Off program has been designed in LabView to prevent further damaging of the test facility.

Functionalities from three different directions of measurement equipment (strain gages); X, Y and Z, have been considered to create a CBM strategy for the test-bearing effective lifetime by measuring the equivalent load.

According to the work load and the time limitation, the building and testing of the test-rig have been dropped out of the thesis. This is in the concern of the supervisors. However, later in this report one will see the necessary details as concerning the building of test facility.

Contents

- 1. INTRODUCTION..... 13
- 2. LITERATURE REVIEW..... 15
 - 2.1. MAINTENANCE..... 15
 - 2.2. CBM TECHNIQUES 16
 - 2.3. MONITORING PARAMETERS FOR PLANT MACHINERY 17
 - 2.4. RECIPROCATING MACHINERY 17
 - 2.5. LINEAR-MOTION MACHINERY 17
- 3. THE TEST-RIG 19
 - 3.1. THE DC MOTOR 20
 - 3.2. THE SHAFT 20
 - 3.3. THE BEARINGS 20
 - 3.4. THE COUPLING 21
 - 3.5. THE BUSHINGS 22
 - 3.6. THE LOAD 22
 - 3.7. The transducer 23
- 4. THE CALCULATIONS 25
 - 4.1. THE SHAFT 25
 - 4.1.1. The critical speed 26
 - 4.1.2. The fatigue..... 27
 - 4.2. THE BEARINGS 31
 - 4.2.1. The cylindrical bearing..... 33
 - 4.2.2. The load bearing..... 34
 - 4.2.3. The test bearing 34
 - 4.2.4. The thrust bearing..... 35
 - 4.3. The Bushing:..... 36
 - 4.4. The Motor Holder:..... 36

4.5.	THE FRICTIONAL MOMENT	37
4.6.	The transducer:	39
4.7.	The FEA of the Transducer:	46
4.8.	The Bolts:	48
4.8.1.	The Axial-bolt:	48
4.8.2.	The Fixture-Screws:	49
4.9.	The Welding:	50
4.10.	The Spring:.....	52
5.	THE DYNAMIC MODEL OF THE SHAFT	53
5.1.	The Dynamic Model:.....	53
5.2.	The Angle of Deflection:.....	56
5.3.	The Critical Speed	58
5.4.	The Reaction Force at Test-bearing.....	59
6.	THE LABVIEW.....	61
7.	THE TEST PROCEDURE.....	63
8.	FURTHER WORK	64
9.	THE CONCLUSION	65
10.	REFERENCES	66
11.	APPENDICES.....	69

List of Tables

Table 1: Condition-Based Maintenance Technology. (1 p. 24)	18
Table 2: The shaft fatigue results	30
Table 3: The bearings type, designation and prices are illustrated.	36
Table 4: The calculation of the estimated frictional moments	37
Table 5: Some of the transducer and SS 4120-24 data	45
Table 6: The summary of calculated stresses and strains in the segments.....	46
Table 7: The elements and material data.....	55
Table 8: The profile calculation.	55
Table 9: The spring stiffness coefficients results.	55

List of Figures

Figure 1: The setup of the test-rig.	19
Figure 2: The shaft view. For more details see sheet No. P-01.....	20
Figure 3: A simplified view of the test-rig to show the location of bearings and bearing-houses.	21
Figure 4: The coupling	21
Figure 5: Elastic coupling from SKF.com.	21
Figure 6: The illustration of the bushing and spring.	22
Figure 7: The illustration of the forces (load) and the reaction-forces A_Y , B_Y & B_X	22
Figure 8: The transducer with some of the dimensions.	23
Figure 9: The transducer with Test-bearing and Bearing house.	23
Figure 10: The radial and axial-load illustration on test-rig.....	24
Figure 11: simplified setup of the shaft and the bearings where $D = 35\text{mm}$ and $d = 20\text{mm}$. ..	25
Figure 12: The illustration of forces on the shaft with sections location due to fatigue criteria.	27
Figure 13: The E295 stress characteristic σN	28
Figure 14: The torsion characteristic.....	28
Figure 15: The distances between the sections with reaction force B_y	30
Figure 16: The simplified setup of test-rig where the position of each bearing is shown by same letter mentioned before.	31
Figure 17: The shaft's free body diagram.	31
Figure 18: a) The transducer setup with blue marked segment 1, b) The shear-forces $V = F_v$, normal-forces $F_N = F'_N$ and moment M_b at the thin wall of segment 1, c) the segment's profile.	39
Figure 19: The profile with dimensions' detail at cross section 1, a) the 2 nd moment of area's illustration, b) the 1 st moment of area's illustration.	40
Figure 20: The transducer setup with blue marked segment 2, b) The shear-forces $V = F_v$, normal-forces F_N and moment M_b at the thin wall of segment 2, c) the segment's profile.	41
Figure 21: The profile with dimensions' detail at cross section 2 and 3, a) the 2 nd moment of area's illustration, b) the 1 st moment of area's illustration.....	42
Figure 22: The transducer setup with blue marked segment 3, b) The shear-forces $V = F_N$, normal-forces F_v and moment M_b at the thin wall of segment 3, c) the segment's profile.....	43

Figure 23: a) The transducer, b) the shear forces diagram, c) the normal forces diagram, d) the bending moment diagram.	44
Figure 24: The loads and constraint application in SolidWorks Simulation.....	46
Figure 25: The mesh distribution.	47
Figure 26: The strain and equivalent stress simulation results.....	47
Figure 27: The illustration of the spring, the Axial and Fixture-bolt(s).....	48
Figure 28: The transducer's screws locations with some of dimensions.	49
Figure 29: The convex welding location on transducer.	50
Figure 30: The illustration of the welding throat area.....	51
Figure 31: The compression spring drawing from Lesjøfors AS.....	52
Figure 32: The modeled shaft in SimulationX.	53
Figure 33: Illustration of the shaft and angle of deflection.	56
Figure 34: the angle of deflection at constraint A.	57
Figure 35: The angle of deflection at constraint B.....	58
Figure 36: The illustration of the shaft's bending occurs because of the critical speed.	59
Figure 37: The deflection of the shaft at the critical speed.	59
Figure 38: The kinematic analysis results at Constraint (B).	60
Figure 39: The steady state results of the kinematic analysis at Constraint (B).	60
Figure 40: The illustration of an automatic switch off control panel in LabView.....	61
Figure 41: The three ports MOSFET circuit. A) The built circuit, B) The correct circuit.....	62
Figure 42: The block diagram of the motor Switch-OFF program with true condition in sub-loop.....	69
Figure 43: block diagram of the motor Switch-OFF program with false condition in sub-loop.	69
Figure 44: The block diagram with false condition in sub-sub-loop.	70
Figure 45: The setup of Input signal.	70
Figure 46: The setup of Output signal.....	71
Figure 47: The acquire signal for Input.....	71
Figure 48: The acquire signal for Output.	72
Figure 49: The Transducer views in Simulation, with Loads and constraints (left), plus mesh (right).....	73
Figure 50: The generated nodes elements and degrees of freedom in Simulation due to Transducer's FEA.	73

Figure 51: Different angles of view of Transducer with the simulated stresses in Simulation.	74
.....	
Figure 52: Different angles of view of Transducer with the simulated strain in Simulation...	75
Figure 53: The setup of dynamic model due to angle deflection criterion.	76
Figure 54: The deflection results for the elements from M1 to M5.....	76
Figure 55: The deflection results for the element from M6 to M10.	76
Figure 56: The setup of dynamic model due to kinematic analysis.	77
Figure 57: The connection of Kinematic drive and with 1 st body element (M1).....	77
Figure 58: The connection of the constraint with the 10 th body element (M10) and the radial load (sphere1).....	77

List of Abbreviations

CBM: Condition based maintenance

MTBF: Meantime between failures

SAE: Society of Automotive Engineers standard J1199 (1979)

FEM: Finite Element Method

FEA: Finite Element Analysis

MBS: Multi Body System

1. INTRODUCTION

This master thesis is a research work into the Condition Based Maintenance for rotating machinery. The part of the rotating system for data acquisition in this research work is the bearings. This thesis is based on the theories acquired and requirement list from an earlier project as a lead up to this thesis. The data will be collected from a test facility under monitoring.

Condition Based Maintenance (CBM) is a process that requires technologies, people, skills and communication to integrate all available equipment condition data. Examples are performance data, maintenance histories, operator logs and design data. This is necessary so as to make timely decisions about the maintenance requirements of major or critical equipments. Condition Based Maintenance uses various process parameters for example pressure, temperature, vibration, flow and material samples like air and oil. (1)

Maintenance of rotating machinery which incorporates bearings is expensive. It is of the interest of all major industries, be it the chemical or the oil industries to reduce such expenses hence the growing interest in condition monitoring. The generation of computer-based monitoring is an important tool for the industry where diagnosis of equipment and malfunctions can help to improve the quality of the produced items.

SKF have been performing condition monitoring on bearings for a long time, nevertheless it is an area of interest to the engineer. Improvements in the design and the optimization of equipments and new machines, requires new forms of monitoring. Bearings are being used in all types of rotating mechanical, electrical and electromechanical machines. (1 p. 175)

The purpose of this study is to provide an in-depth knowledge in Condition Based Maintenance (CBM) on mechanical rotating systems. The Mechatronic Engineer with a vast knowledge in mechanical, control or automated and electrical systems is the right person to work with today's maintenance situation which is Condition Based Maintenance. Condition based maintenance is a condition-driven preventive maintenance program.

This thesis is to build a test facility of rotational system. The rotational system is made of four bearings, a shaft and a 300W DC motor. The bearing is main focus in this CBM thesis; nevertheless the whole mechanical system or structure will also be monitored.

In this task one bearing was run to failure. Out of this the following data was evaluated; equivalent load (fixed load), vibration monitoring using the strain gage connected to the National Instrument (LabView program). CBM strategies were developed based on the data acquired through; Vibration analysis from the bearing and visual observations or physical changes in bearings. Then after mathematical and statistical calculations were computed using various computer programs.

2. LITERATURE REVIEW

This chapter will look at the relevant literature to the project. Firstly, a quick look at maintenance in general. Secondly, a brief literature on Condition Based Maintenance (CBM), its techniques and advantages.

2.1. MAINTENANCE

Maintenance can be described as a science since its execution relies, sooner or later, on most or all of the sciences. Maintenance can also be said to be a philosophy because it must be as carefully fitted to the operation or organization it serves.

The two general classifications of maintenance are: primary functions that demand daily work by the maintenance function and secondary ones assigned to the function for reasons of expediency, know-how, or precedent. Examples of secondary functions are; store keeping, chemical or mechanical plant protection, waste disposal, salvage, insurance administration and other services. (2)

In the early years, maintenance was only performed when something broke or could not function to accomplish the task. This process of addressing equipment failures after the occurrence is called corrective maintenance and still exists today in all industries. But breakdowns and their subsequent impact on future equipment availability calls for a new method or approach to dealing with equipments. (3)

In contrast to corrective maintenance, preventive maintenance is about taking action before total breakdown of the equipment. Under preventive maintenance the following are taken in consideration; period, replacement of parts, and overhauling of the system is taken in consideration. Predictive maintenance or CBM is a part of preventive maintenance.

A side benefit of predictive maintenance is the automatic ability to monitor the meantime-between-failures (MTBF). These data provide the means to determine the most cost-effective

time to replace machinery rather than continue to absorb high maintenance costs. The MTBF of plant equipment is reduced each time a major repair or rebuild occurs. (4 p. 72) MTBF is given mathematically as $\theta = 1/\lambda$, where θ is the MTBF and λ is the constant failure rate. (5 p. 78)

Maintenance within the industry is often built upon a long tradition of a hierarchy in the organizational structure with traditional roles in the decision making. Maintenance is built up around well proven (tried and tested) work routines which are in principle founded from the manufacturers' original recommendations. A traditional work method with a time-based maintenance interval, where the intervals are often founded from conservative recommendations from the manufacturer, but which afterwards have changed, based upon one's own operating experience with the equipment. New technology has enabled better controls and analysis and have been included with routine work, but often been included in already established time-based maintenance programs at the various sites. Condition based maintenance will automatically display the reduction of MTBF over the life of the machine. (6)

2.2. CBM TECHNIQUES

Several techniques exist to design a CBM-system. They may be classified as either model-free techniques or model-based techniques.

- **Model-Free Techniques:**

The model-free techniques attempt to find anomalies in a dynamic system by using hardware redundancies, limit and trend checking of readings coming from sensors, etc. For example methods based on vibration analysis; use information given either from displacement or eddy probes, velocity sensors, or accelerometer sensors. (1 p. 98)

- **Model-Based Techniques:**

The model-based techniques use models that theoretically represent the behavior of the dynamic system to estimate the states and parameters of the model. These theoretical values are compared against the actual outputs of the sensors. The resulting values are further processed to decide if a fault is present in the system and to identify the fault origin. (1 p. 99)

2.3. MONITORING PARAMETERS FOR PLANT MACHINERY

Mechanical equipments which include, all rotating, reciprocating, linear motions and other plant equipment or systems related to moving components or process-related dynamic actions, can be evaluated using vibration monitoring techniques.

Many vibration programs are limited to simple machine set ups, such as pumps and fans. While appropriate for these simple rotating machines, vibration monitoring and analysis also can be used on complex rotating equipment and a variety of continuous-process systems. This classification should include pumps, fans, compressors, motor-generators, conveyors and many other continuous-process machines. (7)

2.4. RECIPROCATING MACHINERY

Vibration analysis is directly applicable to reciprocating machinery; however, modified diagnostic logic must be used to evaluate this type of machine train. Unlike pure rotating machines, the vibration patterns generated by reciprocating machines may not be simple harmonics of a rotating shaft. (4 pp. 122 - 123)

2.5. LINEAR-MOTION MACHINERY

Linear-motion machinery, such as indexing machines, also has a repeatable pattern of motion and forces. Vibration analysis also can be used to evaluate these machines and systems. Timing of vibration patterns in relation to the stroke or linear movement is a key to the evaluation of linear-motion equipment. All data should be recorded and evaluated with an accurate reference to time sequence of the repetitive pattern of movement. (4 pp. 122 - 123)

Table 1: Condition-Based Maintenance Technology. (1 p. 24)

Inputs	Sensor readings are the primary source of information about the state of the system.
	Condition-Based Maintenance
Framework	Identification of system malfunctions must be performed while the system is operating; i.e. there is no need to stop the system to perform diagnosis. CBM neither can stop nor interfere with the operation of the dynamic system under observation
Objectives	Provide assessment of the system condition based on interpretation of sensor data. Provide lead-time and required maintenance prior to predicted failure. Fix or replace a faulty component in a timely manner such that the operational safety of the system is not compromised.
Requirements	Estimation of states and parameters of the system under observation; Detection of system malfunctions, such as component failures or variations in operating conditions; Identification of the origin of any detected fault, its type and characteristics Assessment of system condition and description of its variation in time; Recording of the vital parameters that describe the condition of the system; Forecast expected conditions of the observed system; Suggest repair actions that restore the system to a state in which it can perform its required function
Outputs	Alert the operator when a fault is detected. Notify of a suspected component. Report an assessment of present and future system conditions. Suggest corrective actions.
Benefits	Reduce maintenance costs. Increase equipment reliability. Reduce equipment downtime. Extend service life of the observed system. Provide continuous evaluation of system condition. Increases operational safety. Reduce severity of faults. Attempts to totally eliminate catastrophic failures. Extend maintenance cycles. Reduces technician training requirements

3. THE TEST-RIG

This chapter looks at the description of the test facility setup, forces and limitation. In the previous chapter it have been discussed that there are basically two methods to implement the CBM, namely;

- Model based technique
- Model free technique

This project is based on the model free technique. On the other hand the construction has to satisfy the requirements list from the pre-project work. (8)

The test facility includes:

- The DC motor
- The shaft
- Four bearings with three bearing-houses
- The coupling
- Bushings
- Axial and radial load (see Figure 1)
- The transducer

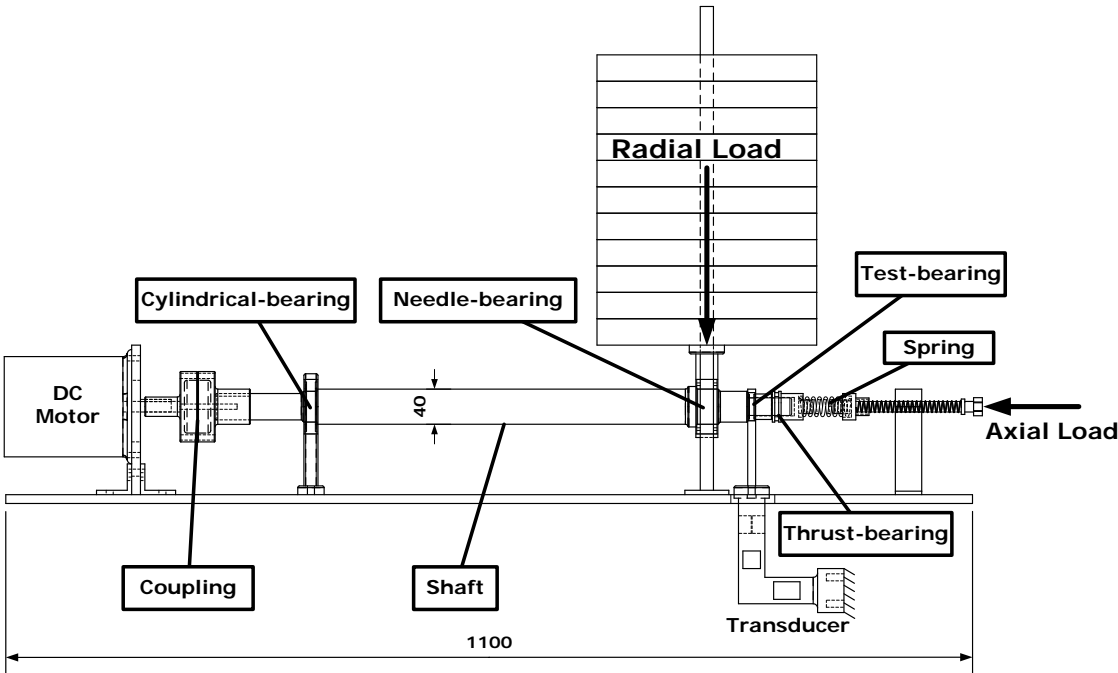


Figure 1: The setup of the test-rig.

3.1. THE DC MOTOR

The DC motor which would be used in test-rig; was produced by *Roley Somer* with 300 W power, 2900 rpm constant speed, 13.5 A current and 22 V voltage. The motor's outer shaft has diameter 12 mm. This DC motor was chosen, based on the pre-estimations done in pre-project. (8)

3.2. THE SHAFT

The shaft was constructed with varying diameters (stepped shaft) with respect to assemble or disassemble the components. The shaft material is E295 (St50-2, Germany standard). (9)

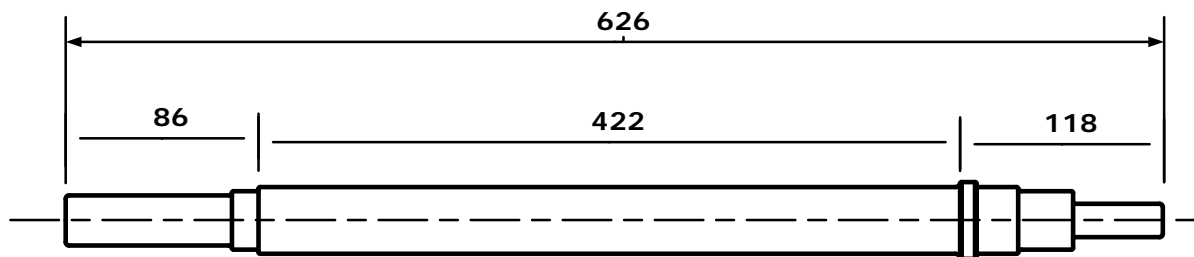


Figure 2: The shaft view. For more details see sheet No. P-01.

3.3. THE BEARINGS

The test-rig contains four different types of bearings:

- The cylindrical bearing (at A)
- The ball bearing (at B)
- The needle bearing (at C) and
- The cylindrical-thrust bearing (at D) (see Figure 3)

The CBM's test is about performing destructive test on the ball bearing B. But the needle and cylindrical-thrust bearing will endure the radial and axial load respectively.

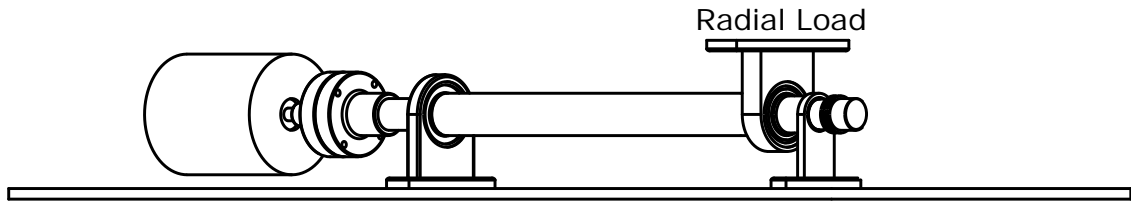


Figure 3: A simplified view of the test-rig to show the location of bearings and bearing-houses.

3.4. THE COUPLING

The coupling will attach the shaft to the DC motor by key-joint and screwed to the both motor's outer shaft and the shaft. And the type is an elastic or flexible coupling which has to be selected from the catalogue (i.e. TOOLS Fag-Verktøy AS) where the motor's outer shaft is 12 mm and the shaft is 30 mm in diameter. (See Figure 1& Figure 4)

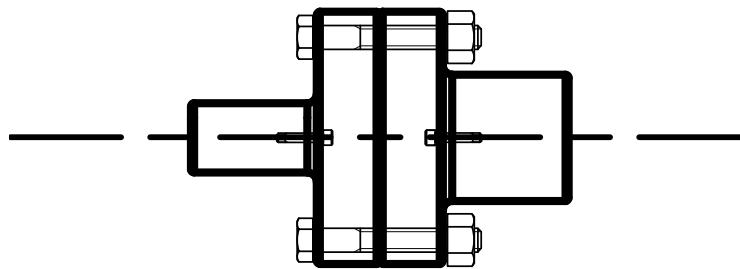


Figure 4: The coupling



Figure 5: Elastic coupling from SKF.com.

3.5. THE BUSHINGS

The test-rig has two bushings where one is located between the ball and the thrust bearing; the other is located between the thrust bearing and the spring. The purpose to have these bushings is to transmit an axial load just to the ball bearing not to the shaft or the rest of the system. (See Figure 6)

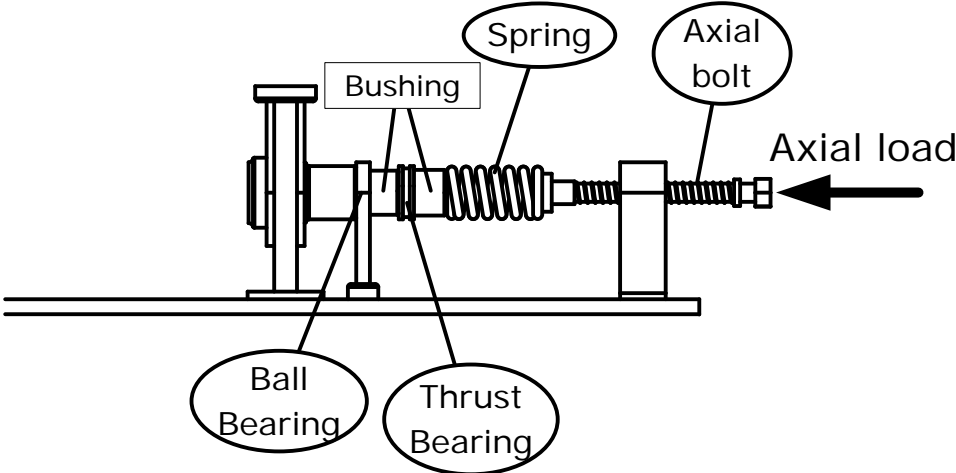


Figure 6: The illustration of the bushing and spring.

3.6. THE LOAD

One of the requirements was to generate enough radial and axial-load to damage at least one roller bearing within 2-3 days. The load value will be evaluated in next chapter.

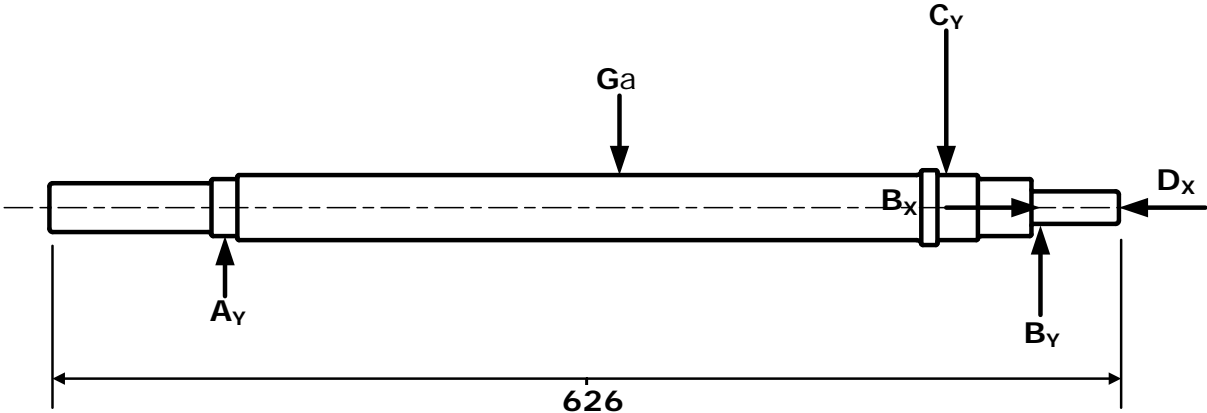


Figure 7: The illustration of the forces (load) and the reaction-forces A_y , B_y & B_x .

3.7. The transducer

The transducer is the part which is fastened beneath of the test-bearing and is constructed to attach some strain-gages in center of the thin quadratic walls to capture the forces and forces-variation in three directions X, Y and Z.

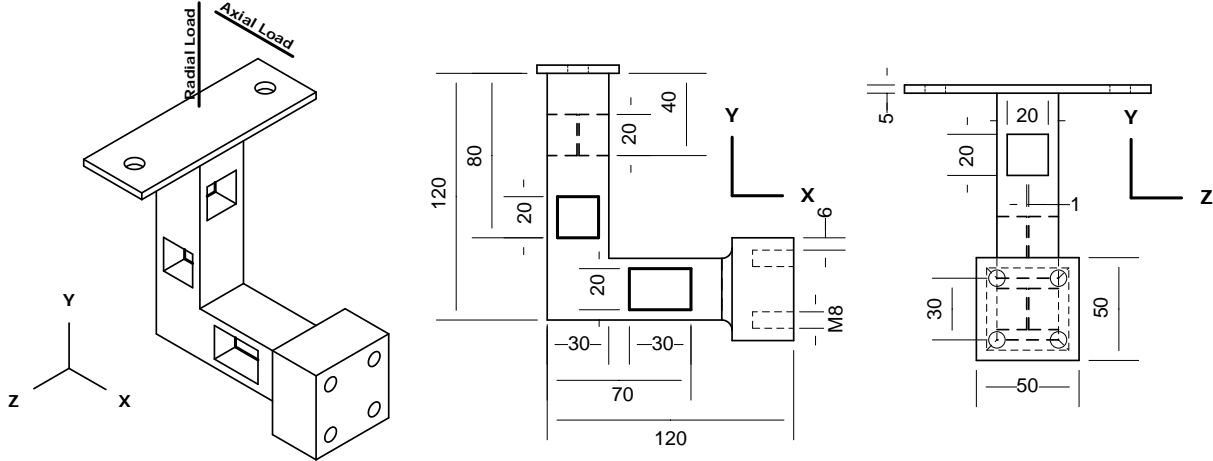


Figure 8: The transducer with some of the dimensions.

The test-rig is designed to carry forces in two directions X & Y where the transducer is able to detect forces in three directions. The third direction detection Z can be useful in purpose to improve the knowledge of the rotational system’s behavior due to CBM research.

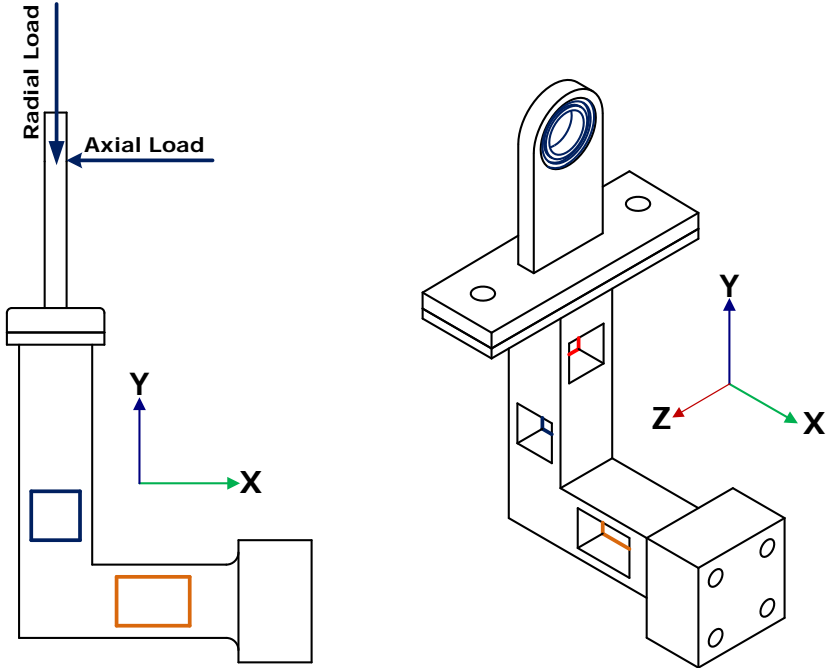


Figure 9: The transducer with Test-bearing and Bearing house.

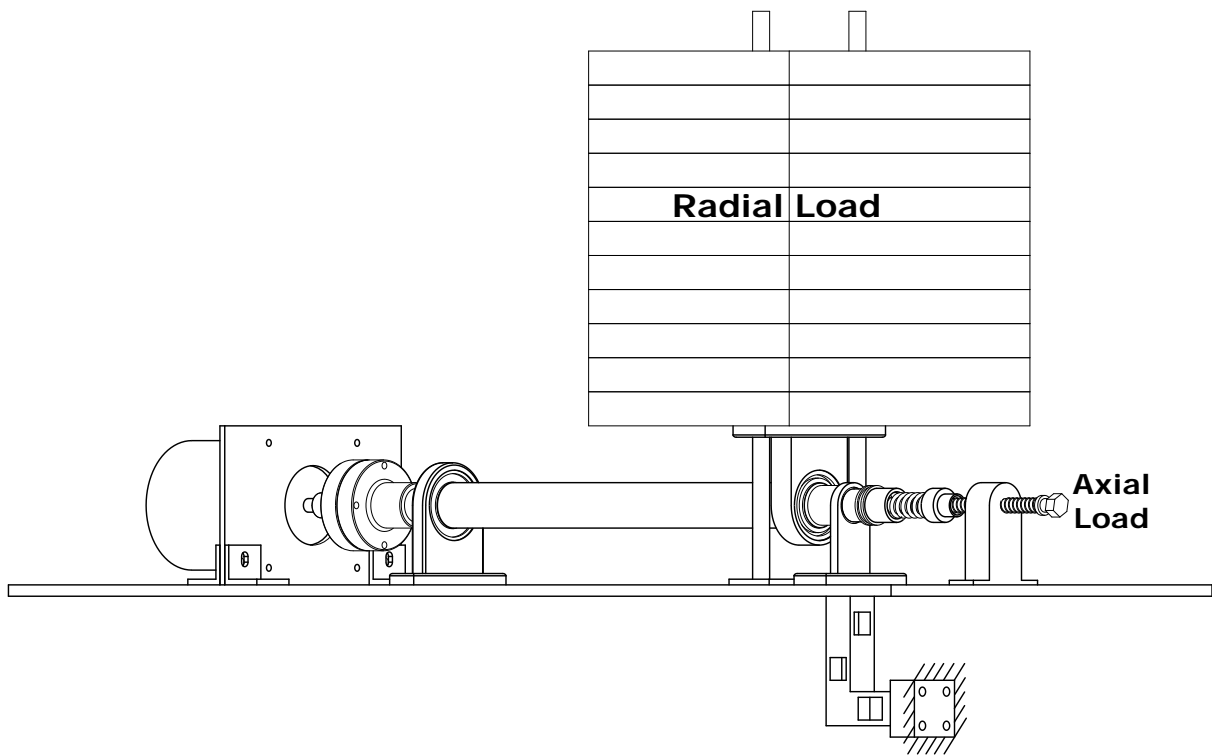


Figure 10: The radial and axial-load illustration on test-rig.

4. THE CALCULATIONS

It is quite obvious that the CBM's test-rig has to be dimensioned based on engineering calculation. The detail calculations are required. This chapter contains the test-rig relevant formulas and calculations are based on Master Mechatronic course material, components' supplier catalogue and material properties.

4.1. THE SHAFT

The chosen material due to the shaft is E295. (9)

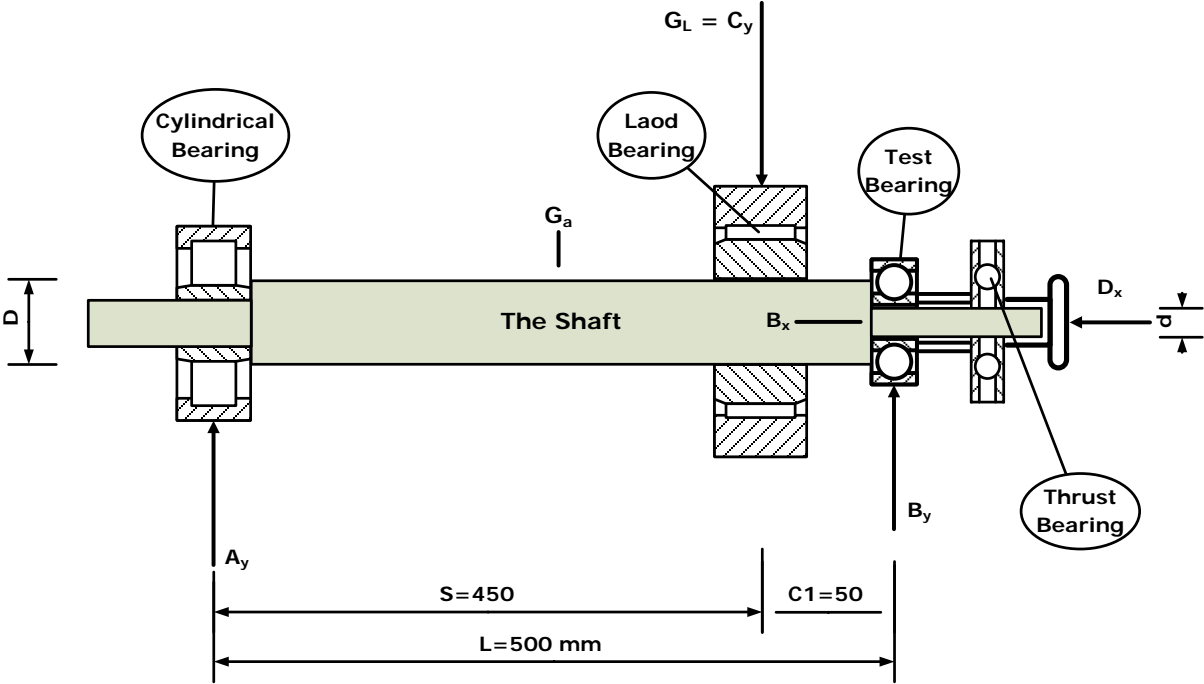


Figure 11: simplified setup of the shaft and the bearings where $D = 35\text{mm}$ and $d = 20\text{mm}$.

Since the construction is meant to be used as a test facility, the safety-factor determined $\eta = 1.5$.

4.1.1. The critical speed

The shaft deflection calculation, where the deflection caused by shaft own weight is:

$$f_{0,a} = \frac{5 \cdot G_a \cdot l_a^3}{384 \cdot E \cdot I_a} = \frac{5 \cdot 37 \text{ N} \cdot (500 \text{ mm})^3}{384 \cdot 210000 \text{ MPa} \cdot 73662 \text{ mm}^4} = 0.0039 \text{ mm} \quad (4-1)$$

Where:

$f_{0,a}$: The deflection caused by shaft own weight [mm].

G_a : The shaft own gravity force [N].

l_a : The shaft length (between two reaction-forces A_y and B_y) [mm].

E : The young modulus [MPa].

I_a : The shaft inertia where $I = \pi \cdot d_a^4 / 64$ [mm⁴] and d_a is the outer massive shaft diameter [mm].

The shaft deflection calculation, where the deflection caused by extern load is:

$$f_{0,l} = \frac{G_l \cdot S^2 \cdot C_1^2}{3 \cdot E \cdot I_a \cdot l_a} = \frac{2946 \text{ N} \cdot 450^2 \text{ mm}^2 \cdot 50^2 \text{ mm}^2}{3 \cdot 210000 \text{ MPa} \cdot 73662 \text{ mm}^4 \cdot 500 \text{ mm}} = 0.0643 \text{ mm} \quad (4-2)$$

Where:

$f_{0,l}$: The deflection caused by external load [mm].

G_l : The load force; $G_l = M_l \cdot g \cdot \eta$ [N].

S : The distance between cylindrical bearing and the load [mm].

C_1 : The distance between the test bearing and the load [mm].

The shaft own critical speed can be calculated by the equation below:

$$n_{cr} = \frac{30}{\pi} \sqrt{\frac{g}{f_0}} \rightarrow \begin{cases} n_{cr,G} = 15149 \text{ rpm} \\ n_{cr,l} = 3732.5 \text{ rpm} \end{cases} \quad (4-3)$$

Where:

n_{cr} : The shaft critical speed [rpm].

$n_{cr,G}$ & $n_{cr,l}$: The shaft critical speed is caused by own gravity & load respectively.

g : The gravity acceleration ($g = 9.81 \text{ m/s}^2$).

f_0 : The shaft static deflection [mm].

The total critical speed can be determined by **Dunkerleys Method**:

$$n_{cr,total} = \sqrt{\frac{1}{\left(\frac{1}{n_{cr,sh}^2}\right) + \left(\frac{1}{n_{cr,l}^2}\right)}} = \sqrt{\frac{1}{\left(\frac{1}{15149^2}\right) + \left(\frac{1}{3732.5^2}\right)}} = 3624 \text{ rpm} \quad (4-4)$$

The actuator rotational speed is $n_{motor} < 0.8 \cdot n_{cr,total}$ with respect to the safety-factor $\eta=1.5$ and considering a uniform shaft with $D = 35 \text{ mm} \rightarrow$ the shaft is OK.

4.1.2. The fatigue

To calculate the shaft's fatigue, would be carried out in the worst case scenario where the shaft's notch is designed. The calculation of section A-A shows below in detail, but the other sections will be represented in Table 2.

The shaft designed with varying diameters and it steps up from the lowest diameter $d = 20$ mm to the highest $D = 46$ mm. But the most critical sections due to the fatigue criteria are where the high forces arise (at C and B), so here will be represented by just four sections (A-A, B-B, C-C and D-D).

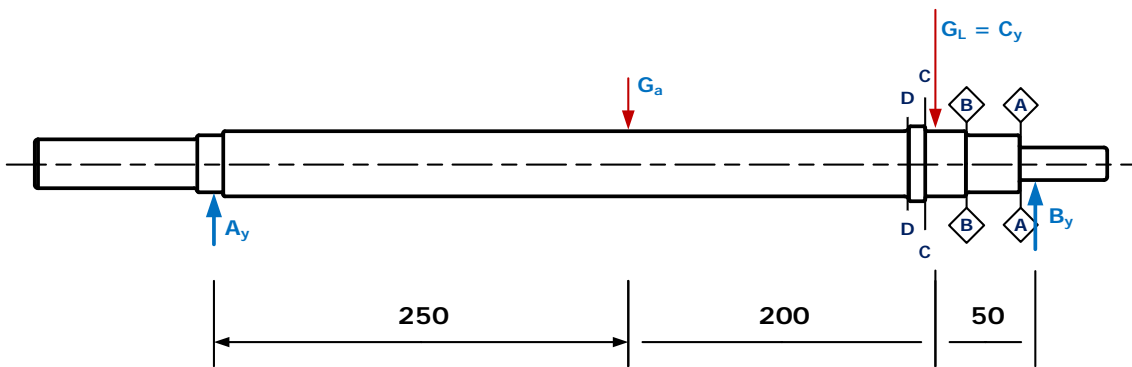


Figure 12: The illustration of forces on the shaft with sections location due to fatigue criteria.

The reaction forces are found by:

$$\sum M_A = 0 \rightarrow G_L \cdot 450\text{mm} + G_a \cdot 250\text{mm} - B_y \cdot 500\text{mm} = 0 \quad (4-5)$$

Where:

M_A : The moment about reaction force at A (A_Y).

$$G_a = \frac{\pi}{4} \cdot \left(\frac{D}{100}\right)^2 \cdot \rho \cdot \frac{L}{100} \cdot g = \frac{\pi}{4} \cdot \left(\frac{35\text{mm}}{100}\right)^2 \cdot 7.85 \frac{\text{kg}}{\text{dm}^3} \cdot \frac{500\text{mm}}{100} \cdot 9.81 \frac{\text{m}}{\text{s}^2} = 37 \text{ N} \quad (4-6)$$

Where:

D: The shaft diameter [mm].

g: The gravity acceleration [m/s^2].

L: The distance between point A and B [mm].

ρ : The material mass density [kg/dm^3].

And:

$$G_L = M_L \cdot g = 200\text{kg} \cdot 9.81 \frac{\text{m}}{\text{s}^2} = 1962 \text{ N} \quad (4-7)$$

Where:

M_L : The mass [kg].

g: The gravity acceleration [m/s²].

$$\mathbf{B}_y = \frac{(\mathbf{G}_L \cdot 450 + \mathbf{G}_a \cdot 250) \cdot \eta}{500} = \frac{(1962 \cdot 450 + 37 \cdot 250) \cdot \eta}{500} = 1786 \cdot \eta = 2676 \text{ N} \quad (4-8)$$

From Newton 2nd law:

$$\sum \mathbf{F}_y = 0 \rightarrow \mathbf{B}_y + \mathbf{A}_y - \mathbf{G}_a - \mathbf{G}_L = 0 \rightarrow \mathbf{A}_y = 301 \text{ N} \quad (4-9)$$

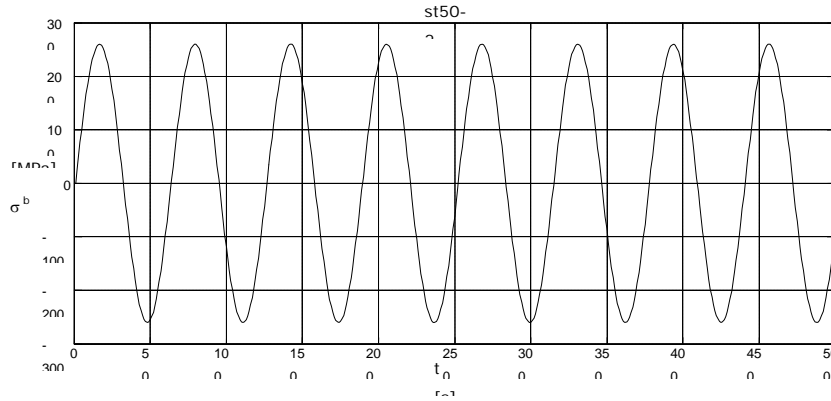


Figure 13: The E295 stress characteristic σ_N .

The bending momentum and torsion stress at section A-A could be calculated such:

$$\mathbf{M}_b = \mathbf{B}_y \cdot \text{arm} = 2676 \cdot 4 = 10704 \text{ Nmm} \quad (4-10)$$

Knowing that the actuator's torque is $T = 1 \text{ Nm}$, so:

$$\tau = \frac{T}{W_p} = \frac{1000 \text{ Nmm} \cdot 16}{\pi \cdot (20 \text{ mm})^3} = 0.64 \text{ MPa} \quad (4-11)$$

Where:

τ : The shear stress [MPa].

W_p : The polar section modulus [mm³], $W_p = \frac{\pi \cdot D^3}{16}$ D is section diameter [mm].

The torsion stress is constant which means that $\tau_a = 0 \text{ MPa}$.

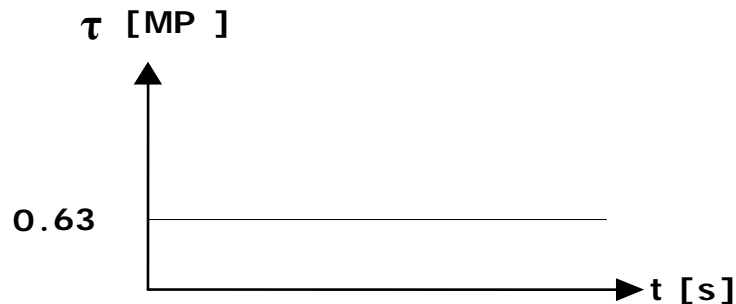


Figure 14: The torsion characteristic.

The bending stress is then:

$$\sigma_b = \frac{M_b}{W} = \frac{10704 \text{ Nmm} \cdot 32}{\pi \cdot 20^3 \text{ mm}^3} = 13.6 \text{ MPa} \quad (4-12)$$

Where:

σ_b : The bending stress [MPa].

M_b : The bending moment [Nmm].

W : The section modulus [mm^3], $W = \frac{\pi \cdot D^3}{32}$ D is section diameter [mm].

The reduction factor b_{tot} is then determined as:

$$b_{\text{tot}} = b_1 \cdot b_2 \cdot b_3 = 0.9 \cdot 0.93 \cdot 1 = 0.837 \quad (4-13)$$

Where:

b_1 : The dimension effect factor.

b_2 : The surface effect factor.

b_3 : The fiber-direction factor.

b_{tot} : The total reduction factor. (10 p. 49 & 50)

The notch factor K_{fb} :

$$K_{fb} = 1 + \eta(K_t - 1) = 1 + 0.68(1.7 - 1) = 1.476 \quad (4-14)$$

The K_t and η could be read from the tables. (10 p. 51 & 54)

The equivalent stress amplitude can be calculated by the equation:

$$\sigma_{ae} = \sqrt{(K_{fb} \cdot \sigma_b)^2 + 3(K_{fv} \cdot \tau_v)^2} = \sqrt{(1.476 \cdot 13.6 \text{ MPa})^2 + 3(0)^2} = 20 \text{ MPa} \quad (4-15)$$

And the equivalent middle stress:

$$\sigma_{em} = \sigma_m \quad (4-16)$$

Since the test-rig is constructed to run continuously so the torsion will be constant then

$\tau_v = 0 \text{ MPa}$ (see Figure 14), and the symmetry will lead to an alternating stretch-pressure stress concentration at the notch area on the shaft, and at the shaft surface will be the highest stress concentration which means that the equivalent amplitude stress equation can be simplified to:

$$\sigma_{ae} = K_{fb} \cdot \sigma_b = 20 \text{ MPa} \quad (4-17)$$

The amplitude stress from the material characteristic:

$$\sigma_a = \pm 260 \text{ MPa} \quad (4-18)$$

(10 p. 47) & (see Figure 13)

So the safety factor due to fatigue is then:

$$n_u = \frac{\sigma_{a(\text{red})}}{\sigma_{ae}} = \frac{b_{\text{tot}} \cdot \sigma_a}{K_{fb} \cdot \sigma_b} = \frac{0.837 \cdot 260 \text{ MPa}}{20 \text{ MPa}} = 10.9 \quad (4-19)$$

The fatigue safety factor at section A-A is $n_u = 6.2$ so the shaft is OK.

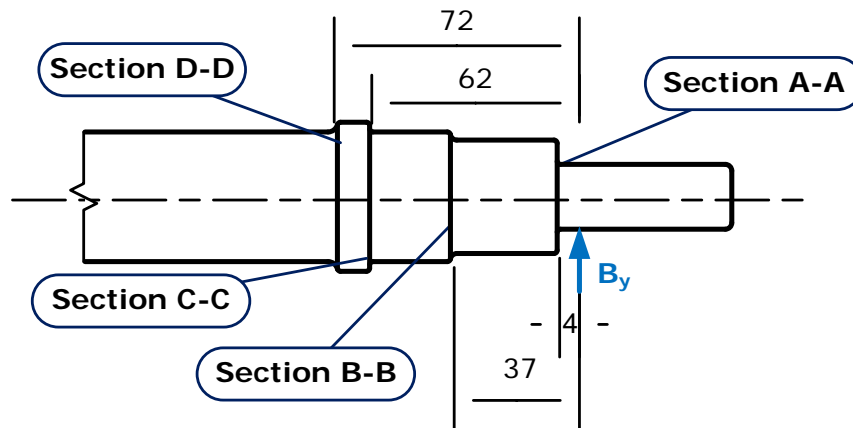


Figure 15: The distances between the sections with reaction force B_y .

The calculation of the other sections has been carried out on the same way shown above and the results are represented in the table below.

Table 2: The shaft fatigue results

Sections	d mm	D mm	r mm	arm mm	M_b Nmm	σ_b MPa	K_{fb}	σ_{ae} MPa	τ MPa	b_{total}	$\sigma_a(\text{red})$ MPa	n_u
A-A	20	35	1	4	10704	13.6	1.47	35	0.637	0.837	217.6	10.9
B-B	35	40	2	37	104130	24.7	1.63	40.3	0.119	0.697	181.4	4.5
C-C	40	46	1	62	165540	39.3	1.90	74.9	0.079	0.651	169.6	2.26
D-D	40	46	3	72	192240	30.6	1.55	47.3	0.079	0.651	169.6	3.58

The fatigue level at the notched area near of the cylindrical bearing, is relatively much lower than the calculated areas and that because of lower reaction force $A_y = 300 \text{ N}$ and the diameter $d = 30 \text{ mm}$ in comparison with the A-A section. (See Figure 12)

4.2. THE BEARINGS

The test-rig is designed to have four bearings. Two of the bearings (cylindrical and load) are fastened to the shaft at A & C. Where the others are just attached to the shaft at B & D (see Figure 16). The selection of bearings due to the test-rig is based on the SKF’s electronic catalogue. From the actuator side the bearings are as follows: (11), (12)

- A: The cylindrical bearing
- B: The test bearing
- C: The load bearing
- D: The thrust bearing

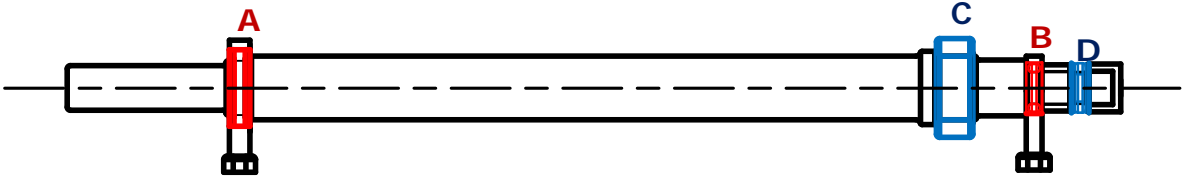


Figure 16: The simplified setup of test-rig where the position of each bearing is shown by same letter mentioned before.

To select the bearings the radial, the axial and the equivalent load (force) for each bearing location has to be determined.

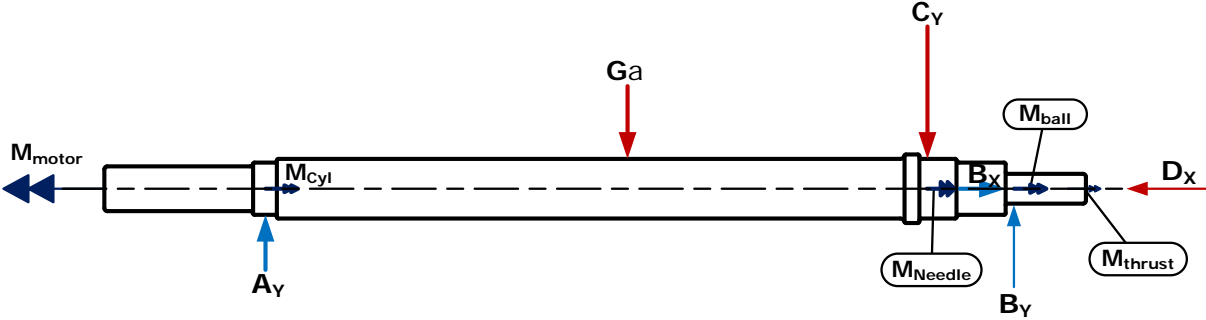


Figure 17: The shaft’s free body diagram.

Compute some of the data:

$$\sum M_A = 0 \rightarrow G_a \cdot \frac{L}{2} + G_l \cdot S - B_y \cdot L = 0 \tag{4-20}$$

Where:

- M_A : The sum moment at A [Nmm].
- G_a : The shaft own gravity load [N].

- G_L : The radial load [N].
 S : The distance from point A to the load [mm].
 L : The distance from point A to point B [mm].
 B_y : The reaction force at point B [N].

And it is assumed that the shaft is a uniform shaft with $D = 35 \text{ mm}$:

$$G_a = \frac{\pi}{4} \cdot \left(\frac{D}{100}\right)^2 \cdot \rho \cdot \frac{L}{100} \cdot g = \frac{\pi}{4} \cdot \left(\frac{35\text{mm}}{100}\right)^2 \cdot 7.85 \frac{\text{kg}}{\text{dm}^3} \cdot \frac{500\text{mm}}{100} \cdot 9.81 \frac{\text{m}}{\text{s}^2} = 37 \text{ N} \quad (4-21)$$

Where:

- D : The shaft diameter [mm].
 g : The gravity acceleration [m/s^2].
 L : The distance between point A and B [mm].
 ρ : The material mass density [kg/dm^3].

And:

$$G_L = M_L \cdot g = 200\text{kg} \cdot 9.81 \frac{\text{m}}{\text{s}^2} = 1962 \text{ N} \quad (4-22)$$

Where:

- M_L : The mass [kg].
 g : The gravity acceleration [m/s^2].

$$G_L \cdot 450\text{mm} + G_a \cdot 250\text{mm} - B_y \cdot 500\text{mm} = 0 \quad (4-23)$$

So:

$$B_y = 1786 \approx 1800 \text{ N} \quad (4-24)$$

$$B_x = D_x = 0.4 \cdot B_y = 720 \text{ N} \quad (4-25)$$

$$\sum F_y = 0 \rightarrow A_y - G_a - G_L + B_y = A_y - 1964 - 37 + 1800 = 0 \quad (4-26)$$

Where:

- F_y : The sum of forces in Y direction [N].

$$A_y = 200 \text{ N} \quad (4-27)$$

$$C_y = G_L = 1962 \text{ N} \quad (4-28)$$

The A_y & C_y are the radial forces at point A & C respectively with safety factor $\eta = 1.5$, but B_y is the reaction force at B considering the safety factor $\eta = 1$. (See Figure 17)

The desired lifetime due to the bearings, is 100 test-bearing's life time such:

$$L_{10,req} = n_{motor} \cdot t_m \cdot t_h \cdot t_d \cdot k = 2900 \cdot 60 \cdot 24 \cdot 2 \cdot 100 = 835.2 \text{ Mrev} \quad (4-29)$$

Where:

$L_{10,req}$: The desired test-rig's lifetime [Mrev].

n_{motor} : The motor's rotational speed $n_{motor} = 2900$ rpm.

t_m : One hour's minutes $m = 60$ min/hour.

t_h : One day's hour $h = 24$ hour/day.

t_d : The test-bearing required lifetime $d = 2$ days.

k : The test-rig required lifetime (except test bearing) $k = 100 \cdot d$.

4.2.1. The cylindrical bearing

To select the cylindrical bearing (at A, Figure 16), the equivalent bearing load is calculated to be:

$$P_u = A_y \cdot \eta = 200 \text{ N} \cdot 1.5 = 300 \text{ N} \quad (4-30)$$

The bearing is selected from SKF's catalogue *NU 1007 ECP*. (13)

Then check the cycle number:

$$L_{10} = \left(\frac{C}{P_u} \right)^{\frac{10}{3}} = \left(\frac{35800 \text{ N}}{300 \text{ N}} \right)^{\frac{10}{3}} = 8366 \text{ Grev} \quad (4-31)$$

To check the system's life time requirement:

$$\frac{L_{10}}{L_{10,req}} = \frac{8366 \text{ Grev}}{835.2 \text{ Mrev}} = 10017 \quad (4-32)$$

From the calculation, the cylindrical bearing's life time $L_{10,cylindrical} \gg 100 L_{10,test-bearing}$ (test bearing life time), hence the selected bearing is **OK**.

4.2.2. The load bearing

The bearing at point C is carrying the payload (see Figure 16). At point C, the equivalent load is then the radial force on the shaft at C (there is no axial load).

$$P_u = C_y \cdot \eta = 1964 \text{ N} \cdot 1.5 = 2946 \text{ N} \quad (4-33)$$

The needle bearing **NA 4908.2R/W64** is selected from SKF catalogue. (14)

Then check the cycle number:

$$L_{10} = \left(\frac{C}{P_u} \right)^{\frac{10}{3}} = \left(\frac{36900 \text{ N}}{2946 \text{ N}} \right)^{\frac{10}{3}} = 4563.7 \text{ Mrev} \quad (4-34)$$

Check the system's lifetime requirement:

$$\frac{L_{10}}{L_{10,req}} = \frac{4563.7 \text{ Mrev}}{835.2 \text{ Mrev}} = 5.5 \quad (4-35)$$

From the calculation, the cylindrical bearing's lifetime $L_{10,cylindrical} > 100 L_{10,test-bearing}$ (test bearing lifetime), hence the selected bearing is **OK**.

4.2.3. The test bearing

The test bearing (at C, see Figure 16) is the only bearing selected:

- To carry both *radial* and *axial* forces.
- With safety factor $\eta \leq 1$.

The equivalent load P_u can be calculated such:

$$P_u = F_r \text{ when } e \leq \frac{F_a}{F_r} \quad (4-36)$$

$$P_u = X \cdot F_r + Y \cdot F_a \text{ when } e > \frac{F_a}{F_r} \quad (4-37)$$

Where:

e , X & Y : SKF factors.

F_r & F_a : The radial and axial force respectively [N].

The values of the X & Y depend on the e and the relationship $f_0 F_a / C_0$, where f_0 is a calculation factor and C_0 is the basic static load rating. (15)

The selected bearing is **61804**. (16)

Then from SKF's data: $C_0 = 32200 \text{ N}$, $f_0 = 15$, but $F_a = 714.45 \text{ N}$ from calculation; so the SKF factors: $X = 1$ & $Y = 0$. Where the equivalent load $P_u = F_r = B_y$ at B. (See Figure 11)

The number of revolution is controlled by the equation: (14)

$$L_{10} = \left(\frac{C}{p_u}\right)^3 = \left(\frac{4030\text{N}}{1800\text{N}}\right)^3 = 11.2\text{Mrev} \quad (4-38)$$

Additionally, the number of estimated operating hours can be calculated by this equation:

$$t = \frac{L_{10}}{\text{rev}} = \frac{11.2 \text{ Mrev}}{174000\text{rev/h}} = 64.4 \text{ hours} \quad (4-39)$$

Where:

rev: Number of motor revolutions per one hour [rev/h].

t: The estimated operation time [hour]. (17)

Based on the **calculation** above the ball bearing (test bearing) estimated to break within 3 days (72 hours operating time) which is acceptable approach according to the requirements.

4.2.4. The thrust bearing

The thrust bearings are constructed to endure only the axial load ($D_x = B_x = 714.5 \text{ N}$). The bearing is selected based on the bore diameter ($d = 20 \text{ mm}$): ***K 81104 TN*** (18)

The bearing's lifetime is controlled where $P_u = B_x \cdot \eta = 720 \cdot 1.5 = 1080 \text{ N}$:

$$L_{10} = \left(\frac{C}{p_u}\right)^{\frac{10}{3}} = \left(\frac{18600 \text{ N}}{1080 \text{ N}}\right)^{\frac{10}{3}} = 13192 \text{ Mrev} \quad (4-40)$$

The test-rig design criterion is checked:

$$\frac{L_{10}}{L_{10,\text{req}}} = \frac{13192 \text{ Mrev}}{835.2 \text{ Mrev}} = 15.8 \quad (4-41)$$

$L_{10,\text{req}}$: The test-rig design criteria is based on motor cycles' number $L_{10,\text{req}} = 806 \text{ Mrev}$.

The selected bearing is OK.

The summary of the bearings' selection, designation and price are represented in Table 3.

Table 3: The bearings type, designation and prices are illustrated.

	Bearing Type	SKF Designation	Tools Ref.	Price [NOK]
A	Cylindrical Bearing	NU 1007 ECP	6109-4885	250,-
B	Ball Bearing	61804	9019-0365	112,-
C	Needle Bearing	NA 4908.2R/W64	6174-0370	444,-
D	Thrust Cylindrical Bearing	K 81104 TN	-	220,-

4.3. The Bushing:

The bushings are exposed to relatively low axial load altitude $F_a = 720$ N and the stress level assumed to be low enough to accept the design without any further calculation. (See Figure 6)

4.4. The Motor Holder:

The DC motor is fixed to the motor holder with four M6×1.25 – SAE 8.8 bolts and the motor holder can be fixed to the board by four angular holders. Since the DC motor torque is $T = 1$ Nm so the mentioned parts concluded to be OK. (See Figure 10 & Sheet No. P-03)

4.5. THE FRICTIONAL MOMENT

The frictional moment could be calculated by the following equation:

$$\mathbf{M = 0.5 \mu P_u d} \quad (4-42)$$

Where:

M: The estimated frictional moment [Nmm]. (19)

μ : Constant coefficient of friction for bearing. (20)

P_u : Equivalent dynamic bearing load [N].

d: Bearing bore diameter [mm].

When for needle roller bearings use F or F_w instead of d.

F: Inner ring raceway diameter [mm].

F_w : Diameter under rollers [mm].

The total estimated frictional moment is the sum of the estimated frictional moment for each bearing:

$$\mathbf{M_{fr,total} = M_{ball} + M_{cyl} + M_{needle} + M_{thrust}} \quad (4-43)$$

Where:

$M_{fr,total}$: The total estimated frictional moment [Nmm].

M_{ball} : The estimated frictional moment for ball bearing [Nmm].

M_{cyl} : The estimated frictional moment for cylindrical bearing [Nmm].

M_{needle} : The estimated frictional moment for needle bearing [Nmm].

M_{thrust} : The estimated frictional moment for cylindrical thrust bearing [Nmm].

Table 4 represents the results of the estimated frictional moment calculation of each bearing.

Table 4: The calculation of the estimated frictional moments

Bearing type	μ	P_u [N]	d [mm]	M [Nmm]
Cylindrical	0.002	300	35	10.5
Needle	0.0025	1964	F = 48	117.8
Ball	0.0015	1800	20	27
Thrust	0.005	720	20	36

$$\mathbf{M_{fr,total} = 10.5 \text{ Nmm} + 117.8 \text{ Nmm} + 27 \text{ Nmm} + 36 \text{ Nmm} = 191.3 \text{ Nmm}} \quad (4-44)$$

To check the motor's ability to run the system, the peak time has to be computed by this equation:

$$t_{\text{peak}} = \frac{\omega}{\alpha} \quad (4-45)$$

Where:

α : Angular acceleration [rad/s²].

ω : Angular speed $\omega = n_{\text{motor}}/(60 \cdot 2\pi)$ [rad/s].

And

$$M_{\text{max}} - M_{\text{fr, total}} = J_{\text{total}} \cdot \alpha \quad (4-46)$$

Where:

M_{max} : The motor max torque [Nm].

$M_{\text{fr, total}}$: The total estimated frictional moment [Nm].

J_{total} : The total mass moment of inertia $J_{\text{total}} = \sum \frac{1}{2} \cdot m_i r_i^2$ [kg-m²].

The selected DC motor MBTE type is produced according to a special order which means out of the producer's catalogue, and there is no access to its data. The maximum torque M_{max} value has been estimated based on the knowledge in limitation of heat exchanging due to DC motor. And the M_{max} value is estimated to be 4 times larger than the continuously torque $T = 1$ Nm.

$$\alpha = \frac{M_{\text{max}} - M_{\text{fr, total}}}{J_{\text{total}}} = \frac{3.8087 \text{ Nm}}{0.01936 \text{ kgm}^2} = 197.3 \frac{\text{rad}}{\text{s}^2} \quad (4-47)$$

The angular speed:

$$\omega = \frac{2900 \cdot 2\pi}{60} = 304 \frac{\text{rad}}{\text{s}} \quad (4-48)$$

The peak time:

$$t_{\text{peak}} = \frac{\omega}{\alpha} = \frac{304}{197.3} = 1.5 \text{ s} \quad (4-49)$$

The peak time 1.5 s shows that the DC motor is powerful enough to run the test.

4.6. The transducer:

The design of the transducer requires the determination of the stresses level (shear-stress, normal-stress) at the critical segments such the center of the thin walls where the strain gauges will be located on both sides of the thin wall. So the following quantities; the shear forces, normal-forces and bending moment at each point is to be computed.

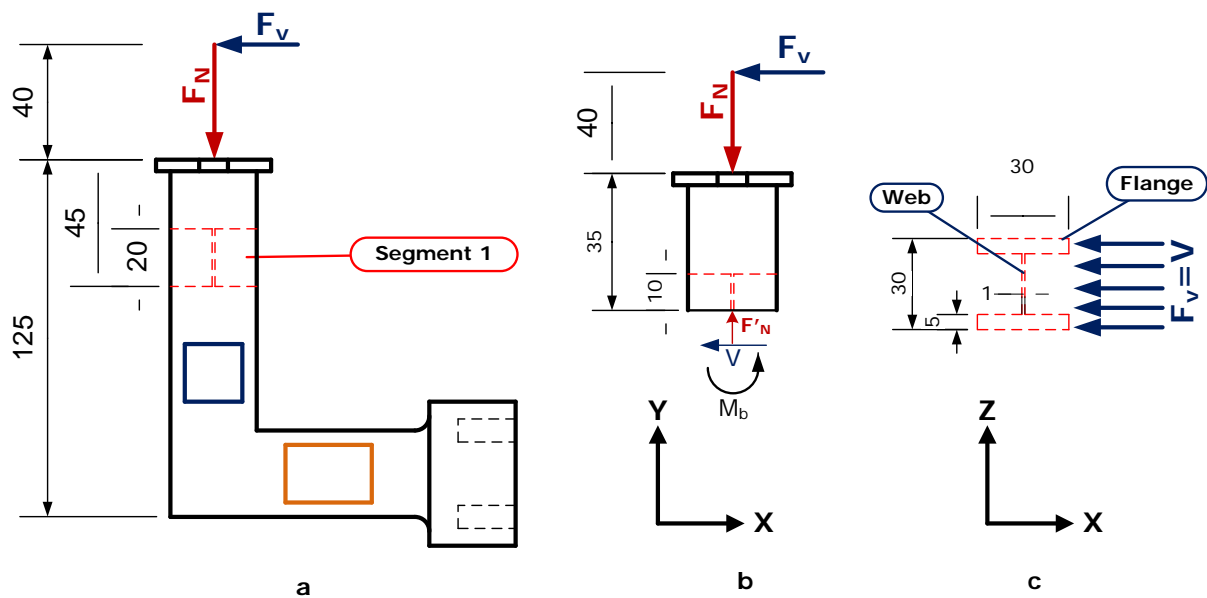


Figure 18: a) The transducer setup with blue marked segment 1, b) The shear-forces $V = F_v$, normal-forces $F_N = F'_N$ and moment M_b at the thin wall of segment 1, c) the segment's profile.

So we need to find the profile's 2nd moment of area "I" such:

$$\begin{aligned} I_1 &= \frac{b_f \cdot h_f^3}{12} = \frac{5 \cdot 30^3}{12} = 11250 \text{ mm}^4 \\ I_2 &= \frac{b_w \cdot h_w^3}{12} = \frac{20 \cdot 1^3}{12} = 1.67 \text{ mm}^4 \\ I &= 2 \cdot I_1 + I_2 = 22500 \text{ mm}^4 \end{aligned} \tag{4-50}$$

Where:

I: The profile's 2nd moment of area [mm^4].

b_f & h_f : the width and height of the flange [mm].

b_w & h_w : The width and height of the web [mm]. (See Figure 19 - a)

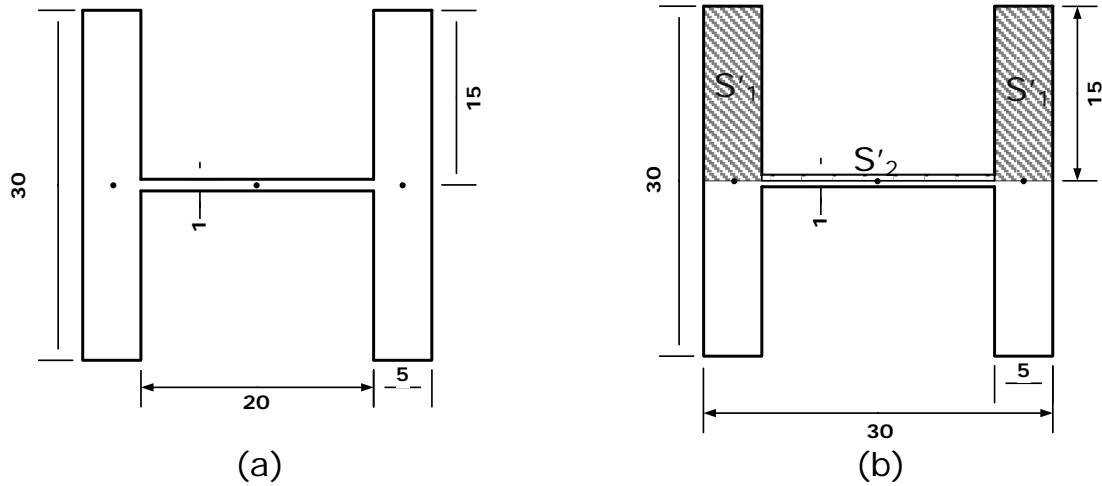


Figure 19: The profile with dimensions' detail at cross section 1, a) the 2nd moment of area's illustration, b) the 1st moment of area's illustration.

The normal stress at segment 1 can be computed by the Navier's equation:

$$\sigma_N = \frac{F_N}{A} + \frac{M_b}{I} y = \frac{1800N}{320\text{mm}^2} + \frac{720N \cdot 75\text{mm}}{22500\text{mm}^4} \cdot 15\text{mm} = 41.6 \text{ MPa} \quad (4-51)$$

Where:

σ_N : The normal stress [MPa]. (21 p. 221)

F_N : The normal forces = Radial forces [N].

A : The profile or cross-section area [mm^2].

M_b : The bending moment at the section [Nmm]. (See Figure 18 - b)

y : The distance from the profile center of mass to the top of the flanges [mm].

The 1st moment of area at the flange of segment 1:

$$S'_1 = y'_1 \cdot A_1 = 7.5 \text{ mm} \cdot (5 \text{ mm} \cdot 30 \text{ mm}) = 1125 \text{ mm}^3 \quad (4-52)$$

Where:

y'_1 : The distance from flange center of mass to the fragment center of mass [mm].

A_1 : The flange area [mm^2].

The maximum shear stress at segment 1 (See Figure 19 - b):

$$\tau_1 = \frac{V \cdot S'_1}{I \cdot t_f} = \frac{720 \text{ N} \cdot 1125 \text{ mm}^3}{22500 \text{ mm}^4 \cdot 10 \text{ mm}} = 3.6 \text{ MPa} \quad (4-53)$$

Where:

τ_1 : The shear stress [MPa]. (21 p. 207)

V : The shear force $V = F_v$ [MPa].

t_f : The width/thickness of the flange [mm].

The calculation of stresses at segment 2:

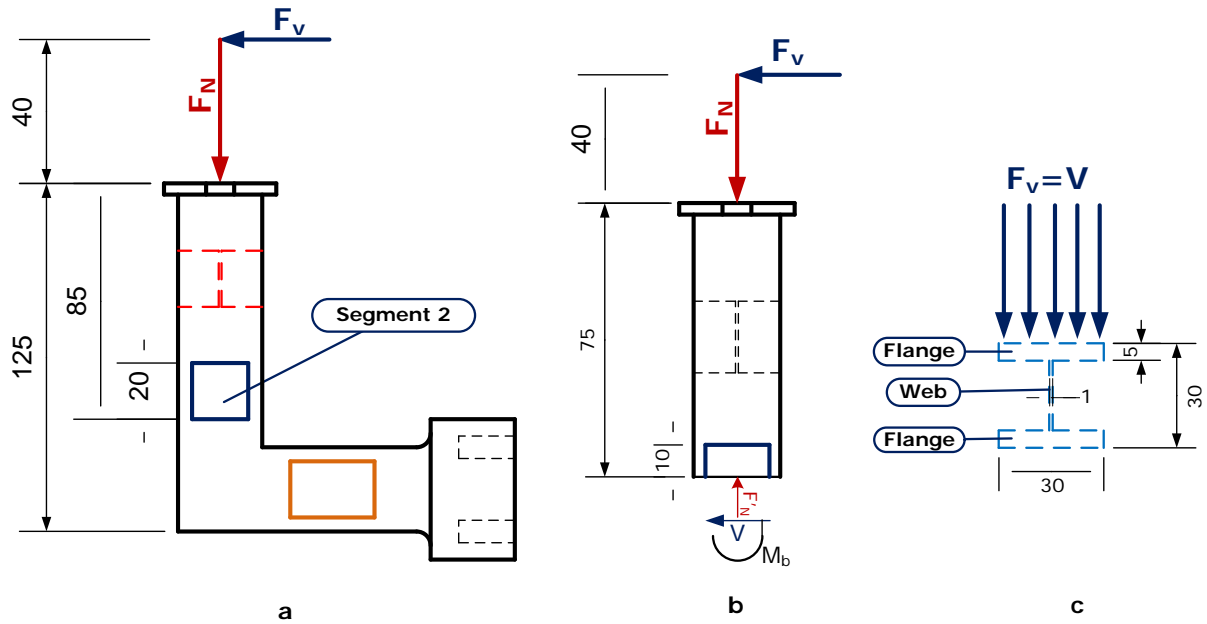


Figure 20: The transducer setup with blue marked segment 2, b) The shear-forces $V = F_v$, normal-forces F_N and moment M_b at the thin wall of segment 2, c) the segment's profile.

The 2nd moment of area “I” due to segment 2:

$$\begin{aligned}
 I_1 &= \frac{b_f \cdot h_f^3}{12} + y_2^2 \cdot A = \frac{30 \cdot 5^3}{12} + 12.5^2 \text{ mm}^2 \cdot 150 \text{ mm}^2 = 23750 \text{ mm}^4 \\
 I_2 &= \frac{b_w \cdot h_w^3}{12} = \frac{1 \cdot 20^3}{12} = 667 \text{ mm}^4 \\
 I &= 2 \cdot I_1 + I_2 = 48167 \text{ mm}^4
 \end{aligned}
 \tag{4-54}$$

Where:

y_2 : The distance from the profile center mass to flange center mass [mm].

A: The cross section area [mm²].

The normal stress at segment 2 can be computed:

$$\sigma_N = \frac{F_N}{A} + \frac{M_b}{I} y = \frac{1800 \text{ N}}{320 \text{ mm}^2} + \frac{720 \text{ N} \cdot 115 \text{ mm}}{48167 \text{ mm}^4} \cdot 15 \text{ mm} = 31.4 \text{ MPa}
 \tag{4-55}$$

The 1st moment of area for the flange of segment 2:

$$S'_1 = y'_1 \cdot A_1 = 12.5 \text{ mm} \cdot (30 \text{ mm} \cdot 5 \text{ mm}) = 1875 \text{ mm}^3
 \tag{4-56}$$

Where:

y'_1 : The distance from flange center of mass to the fragment center of mass [mm].

A_1 : The flange area [mm²].

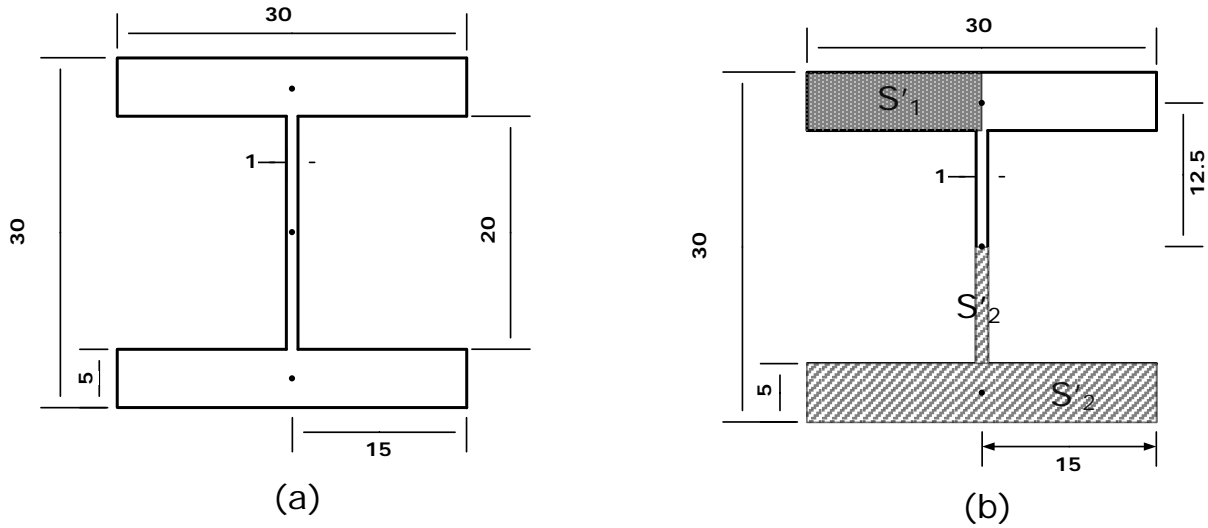


Figure 21: The profile with dimensions' detail at cross section 2 and 3, a) the 2nd moment of area's illustration, b) the 1st moment of area's illustration.

The maximum shear stress at segment 2 (See Figure 21 - b):

$$\tau_1 = \frac{v \cdot S'_1}{I \cdot t_f} = \frac{720 \text{ N} \cdot 1875 \text{ mm}^3}{48167 \text{ mm}^4 \cdot 5 \text{ mm}} = 5.6 \text{ MPa} \quad (4-57)$$

The 1st moment of area due to web:

$$S'_2 = y'_1 \cdot A_1 + \frac{1}{2} \cdot t_w \cdot \left(\frac{h_w^2}{4} - y_2^2 \right)$$

$$S'_2 = 1875 + \frac{1}{2} \cdot 1 \text{ mm} \cdot (100 - y_2^2) \begin{cases} y_2 = 0 \rightarrow S'_{2,\max} = 1925 \text{ mm}^3 \\ y_2 = \frac{h_w}{2} \rightarrow S'_{2,\min} = 1875 \text{ mm}^3 \end{cases} \quad (4-58)$$

Where:

y_2' : The distance from web center of mass to the flange [mm].

t_w : The web thickness [mm].

The maximum shear stress at segment 2 (See Figure 21 - b):

$$\tau_{2,\max} = \frac{v \cdot S'_2}{I \cdot t_w} = \frac{720 \text{ N} \cdot 1925 \text{ mm}^3}{48167 \text{ mm}^4 \cdot 1 \text{ mm}} = 29 \text{ MPa} \quad (4-59)$$

The calculation of stresses at segment 3:

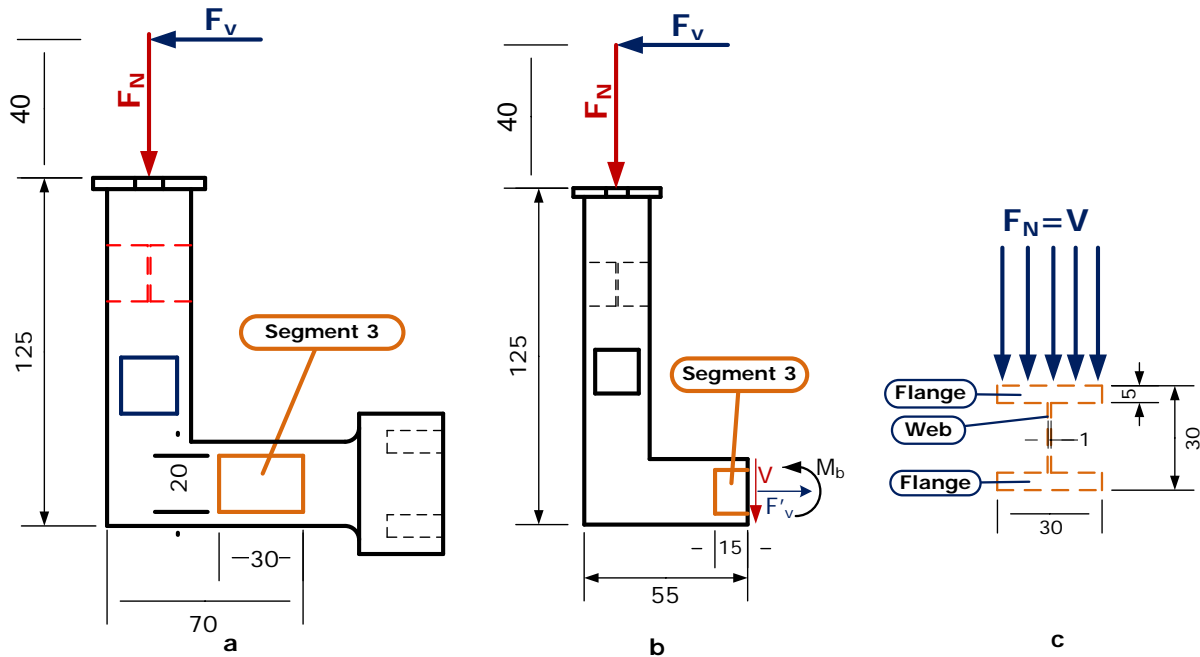


Figure 22: The transducer setup with blue marked segment 3, b) The shear-forces $V = F_N$, normal-forces F_v and moment M_b at the thin wall of segment 3, c) the segment's profile.

The 2nd moment of area "I" due to segment 3:

$$\begin{aligned}
 I_1 &= \frac{b_f \cdot h_f^3}{12} + y_2^2 \cdot A = \frac{30 \cdot 5^3}{12} + 12.5^2 \text{ mm}^2 \cdot 150 \text{ mm}^2 = 23750 \text{ mm}^4 \\
 I_2 &= \frac{b_w \cdot h_w^3}{12} = \frac{1 \cdot 20^3}{12} = 667 \text{ mm}^4 \\
 I &= 2 \cdot I_1 + I_2 = 48167 \text{ mm}^4
 \end{aligned}
 \tag{4-60}$$

Where:

y_2 : The distance from the profile center mass to flange center mass [mm].

A: The cross section area [mm²].

The normal stress at segment 3 can be computed:

$$\sigma_N = \frac{F_v}{A} + \frac{M_b}{I} y = \frac{720 \text{ N}}{320 \text{ mm}^2} + \frac{(1800 \text{ N} \cdot 40 \text{ mm} + 720 \text{ N} \cdot 160 \text{ mm})}{48167 \text{ mm}^4} \cdot 15 \text{ mm} = 60.5 \text{ MPa}
 \tag{4-61}$$

The 1st moment of area for the flange of segment 3:

$$S'_1 = y'_1 \cdot A_1 = 12.5 \text{ mm} \cdot (30 \text{ mm} \cdot 5 \text{ mm}) = 1875 \text{ mm}^3
 \tag{4-62}$$

Where:

y'_1 : The distance from flange center of mass to the fragment center of mass [mm].

A_1 : The flange area [mm²].

The maximum shear stress at segment 3 (See Figure 21 - b):

$$\tau_1 = \frac{V \cdot S'_1}{I \cdot t_f} = \frac{1800 \text{ N} \cdot 1875 \text{ mm}^3}{48167 \text{ mm}^4 \cdot 5 \text{ mm}} = 14 \text{ MPa} \quad (4-63)$$

The 1st moment of area due to web:

$$S'_2 = y'_1 \cdot A_1 + \frac{1}{2} \cdot t_2 \cdot \left(\frac{h_w^2}{4} - y_2^2 \right)$$

$$S'_2 = 1875 + 0.5 \cdot 1 \text{ mm} \cdot (100 - y_2^2) \begin{cases} y_2 = 0 \rightarrow S'_{2,\max} = 1925 \text{ mm}^3 \\ y_2 = \frac{h_w}{2} \rightarrow S'_{2,\min} = 1875 \text{ mm}^3 \end{cases} \quad (4-64)$$

Where:

y'_2 : The distance from web center of mass to the flange [mm].

A_2' : The web area [mm²].

t_2 : The web thickness [mm].

The maximum shear stress at segment 3 (See Figure 21 - b):

$$\tau_{2,\max} = \frac{V \cdot S'_2}{I \cdot t_w} = \frac{1800 \text{ N} \cdot 1925 \text{ mm}^3}{48167 \text{ mm}^4 \cdot 1 \text{ mm}} = 72 \text{ MPa} \quad (4-65)$$

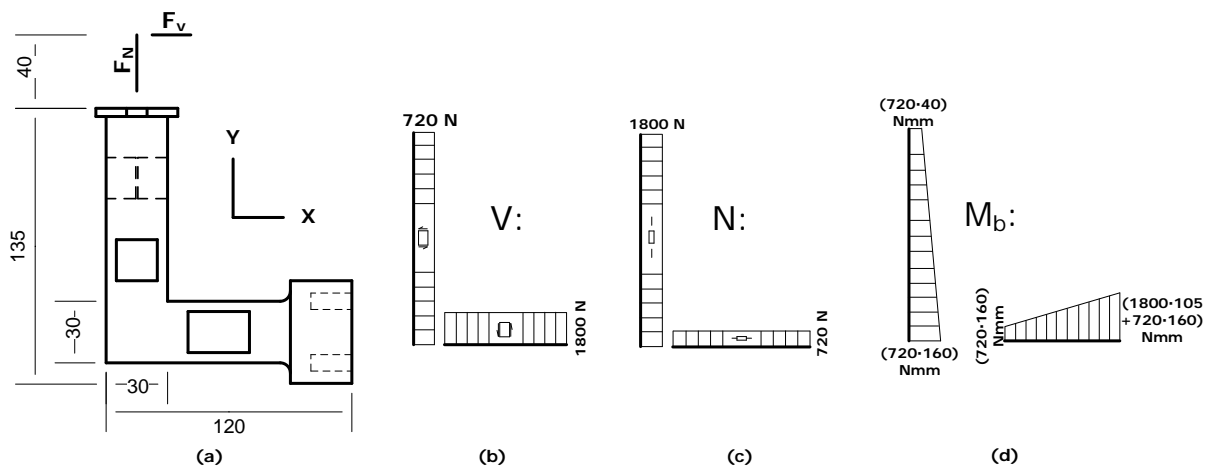


Figure 23: a) The transducer, b) the shear forces diagram, c) the normal forces diagram, d) the bending moment diagram.

The Strain:

The expected strain at the thin walls is calculated by the equation:

$$\epsilon_{45^\circ} = \frac{\tau_{\max}}{2 \cdot \left(G = \frac{E}{2(1+\nu)}\right)} = \frac{1}{2 \cdot \gamma} \quad (4-66)$$

Where:

ϵ_{45° : The measured strain. (22 p. 258)

τ_{\max} : The maximum shear stress at the thin wall [MPa].

G: The modulus of rigidity [GPa].

E: The modulus of elasticity [GPa].

ν : Poisson's ratio.

γ : The shear deformation angle [°].

The transducer's selected material is **SS 4338-06**. (23 pp. 376 - 377)

The force F can also be determined from the measured strain ϵ_{45° . The following relationship applies: (22 p. 260)

$$F = \frac{2\epsilon_{45^\circ} \cdot G \cdot A}{c_A} = \frac{\tau_{\max} \cdot A}{c_A} \quad (4-67)$$

Where:

F: The force [N].

c_A : The cross sectional shape factor of the beam.

A: The cross sectional area [mm²].

But the expected measured strain for the full bridge circuit can be computed by following equation: (22 p. 258)

$$\epsilon_i = \frac{2 \cdot \tau_{\max}}{G} = 4 \cdot \epsilon_{45^\circ} \quad (4-68)$$

Where:

ϵ_i : The measured strain from the full bridge strain gages circuits.

Table 5: Some of the transducer and SS 4120-24 data

A [mm ²]	E [GPa]	G [GPa]	ν
320	70	27	0.29

Table 6: The summary of calculated stresses and strains in the segments

Segment	σ_N [MPa]	$\tau_{1,max}$ [MPa]	$\tau_{2,max}$ [MPa]	ϵ_{45}
1	41.6	3.6	-	-
2	31.4	5.6	29	5E-4
3	60.5	14	72	0.001

4.7. The FEA of the Transducer:

The SolidWorks Simulation program from Dassault Systems is FEA software which can calculate the deflections, the equivalent stresses, the natural frequency and etc. with high accuracy by using FEM. In this project, the transducer has been investigated by Simulation program in purpose to control both the equivalent stresses and the strain levels at the segments area (thin walls) where the strain gages will be attached to.

The transducer will be expanded for static analysis, and the volume elements type of 2nd order has been selected to achieve higher accurate results. The material properties were defined such as Young modulus E, the mass density, the Poisson's ratio and the Yield's strength of **SS4338-06** in Simulation. (23 pp. 376 - 377) Then by applying the forces (radial and axial loads) by choosing the **Force** option for the radial load and the **Remote load** for axial load. The Fixed Geometry option was selected to define the constraint or the boundary conditions at the fixture screws locations. (See Figure 24)

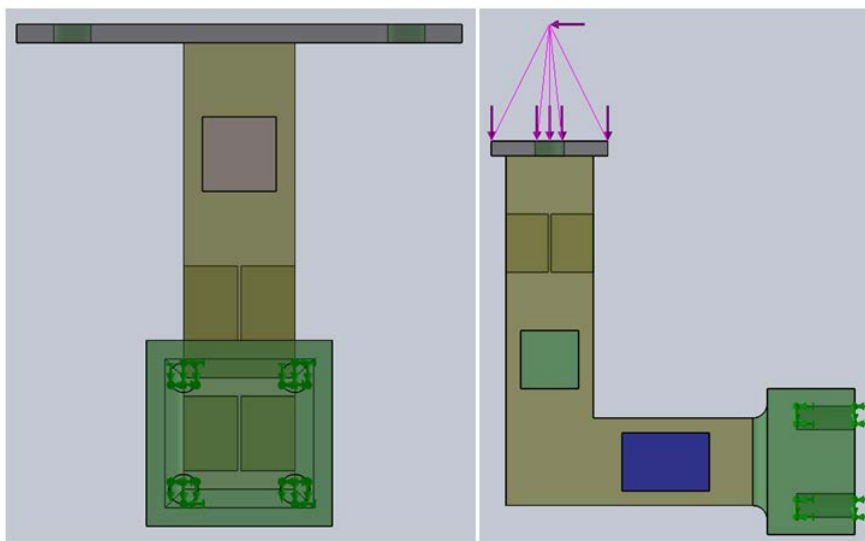


Figure 24: The loads and constraint application in SolidWorks Simulation.

Then the mesh have been applied by selecting moderate mesh size to reduce the computation time, and applying finer mesh at the thin walls' area to achieve better results, even though the mesh generates statistically **66505** nodes, **41915** elements and **197859** degrees of freedom. (See Appendix B - Figure 50)

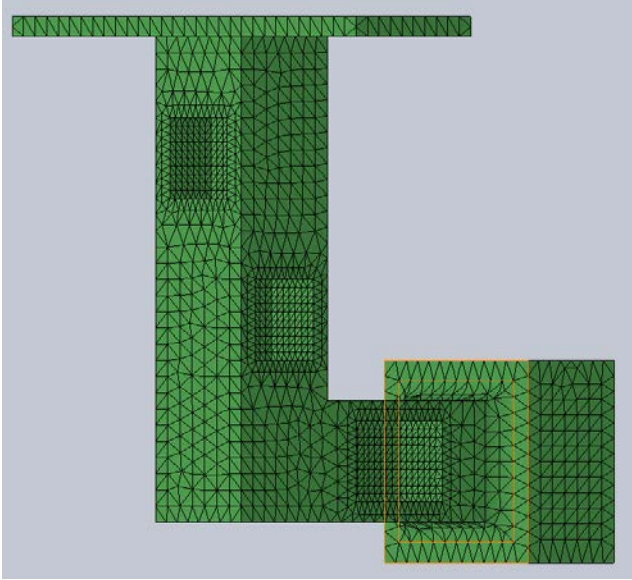


Figure 25: The mesh distribution.

Finally the program has been run to gain the simulation analysis results.

Note that the welding area between the top bracket and the transducer is not considered in this simulation.

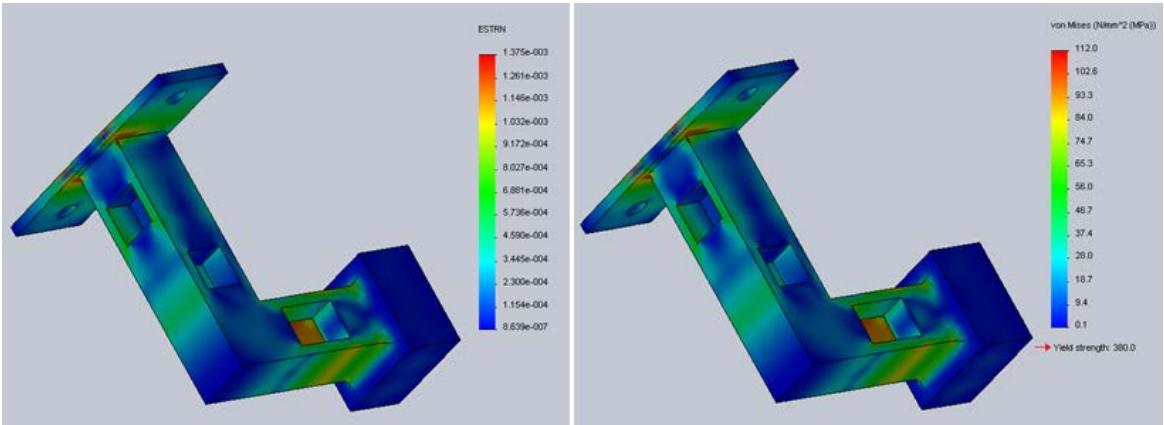


Figure 26: The strain and equivalent stress simulation results.

The equivalent stress level is about 112 MPa at the thin walls of the segments which is below the yield's stress, so therefore the transducer is **OK**.

4.8. The Bolts:

4.8.1. The Axial-bolt:

The axial-bolt generates the axial load due to test bearing according to the system’s load requirements. This chapter will present the leading calculation to select the bolt’s type and dimensions based on **NS 1074 part 1** standard. (10 pp. 157 - 173)

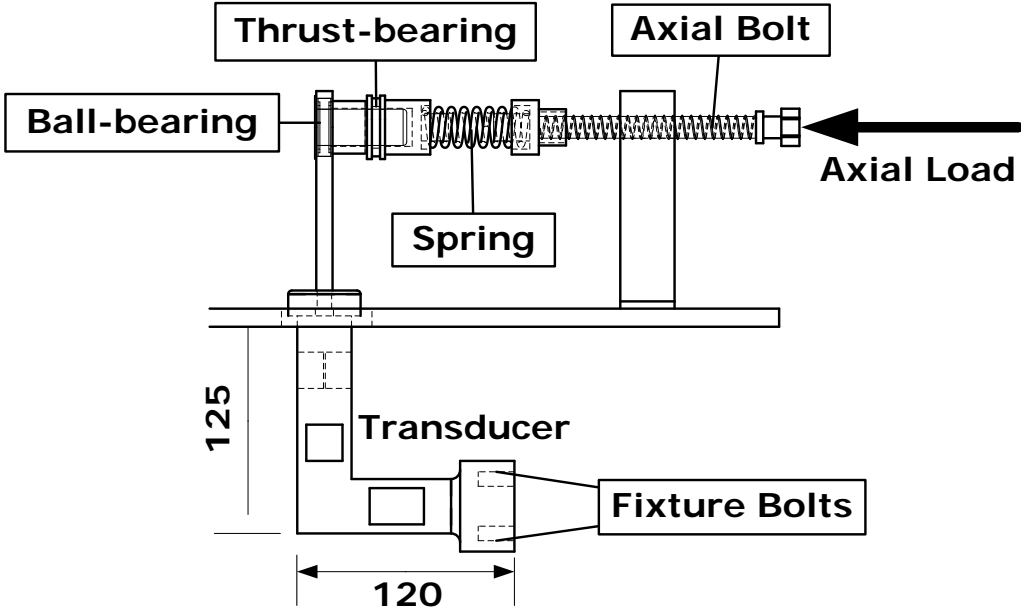


Figure 27: The illustration of the spring, the Axial and Fixture-bolt(s).

The axial bolt will be exposed to an axial force and the stress can be calculated where the bolt is M16 due to metric standard:

$$A_t = \frac{\eta \cdot F}{S_p} = \frac{6 \cdot 720 \text{ N}}{310 \text{ MPa}} = 14 \text{ mm}^2 \tag{4-69}$$

Where:

- S_p: The proof strength with SAE class 4.8 [MPa]. (24 p. 408)
- F_a: The axial force [N].
- η: The safety factor η = 6.
- A_t: The bolt stress area [mm²].

The selected bolt is M16 × 2 – SAE 4. 8.

4.8.2. The Fixture-Screws:

The transducer will be fastened by four fixture-bolts to the disk frame to hold the test-bearing house in its position.

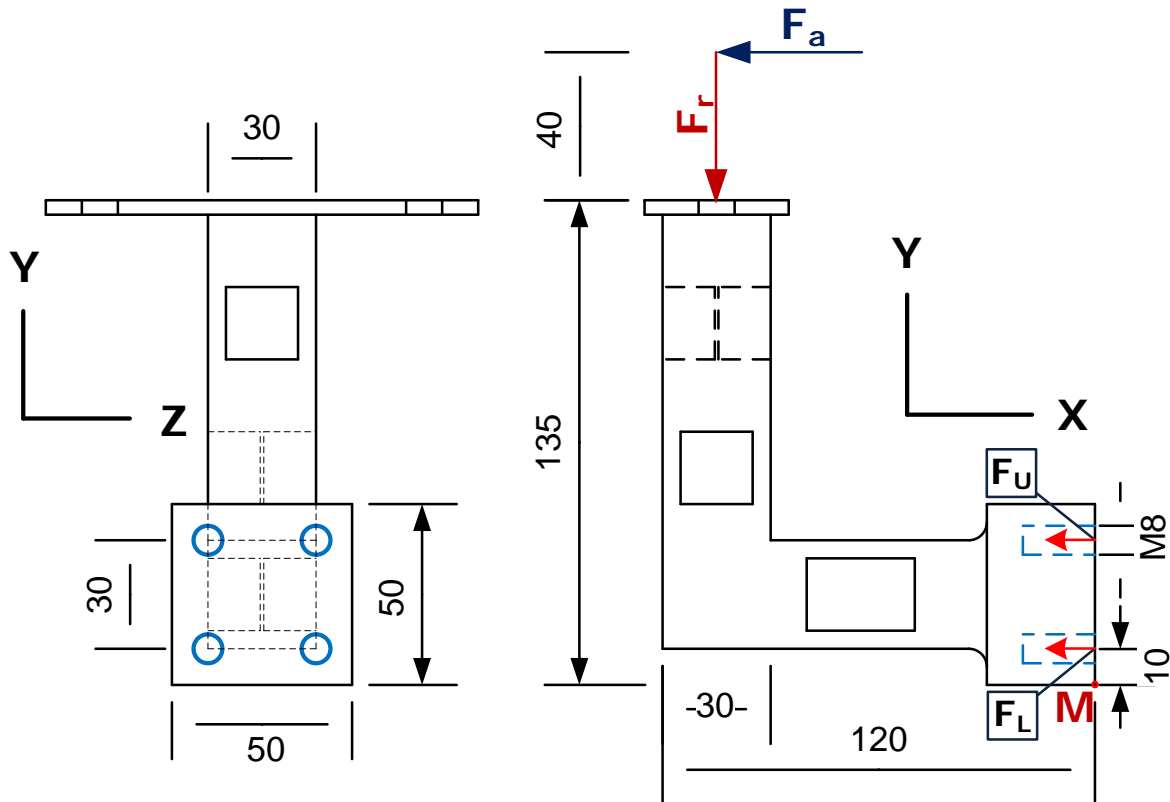


Figure 28: The transducer's screws locations with some of dimensions.

To select the screws, the forces F_U & F_L has to be calculated and that is done by computing the sum of moment at point M such:

$$\begin{aligned} \sum M_M &= 0 \\ F_r \cdot 105\text{mm} \cdot \eta + F_a \cdot 175\text{mm} \cdot \eta &= 2 \cdot F_U \cdot 40\text{mm} + 2 \cdot F_L \cdot 10\text{mm} \\ 1260000 &= 85 \cdot F_U \rightarrow F_U = 14824 \text{ N} \end{aligned} \quad (4-70)$$

Where:

- F_r : The radial force [N].
- F_a : The axial force [N].
- η : The safety factor $\eta = 4$.
- F_U : The load to upper screws [N].
- F_L : The load to lower screws [N].

The stress area was found:

$$A_t = \frac{F_U}{S_p} = \frac{14824\text{N}}{600\text{MPa}} = 25 \text{ mm}^2 \quad (4-71)$$

Where:

A_t : The stress area [MPa].

S_p : The proof strength [MPa].

The selected screw is **M8 × 1.25 – SAE 8.8**. (24 p. 388 & 408)

4.9. The Welding:

The top bracket and the transducer are welded together by convex fillet welds along the sides, each of which is $l = 30 \text{ mm}$ long with $a = 4 \text{ mm}$ throat length.

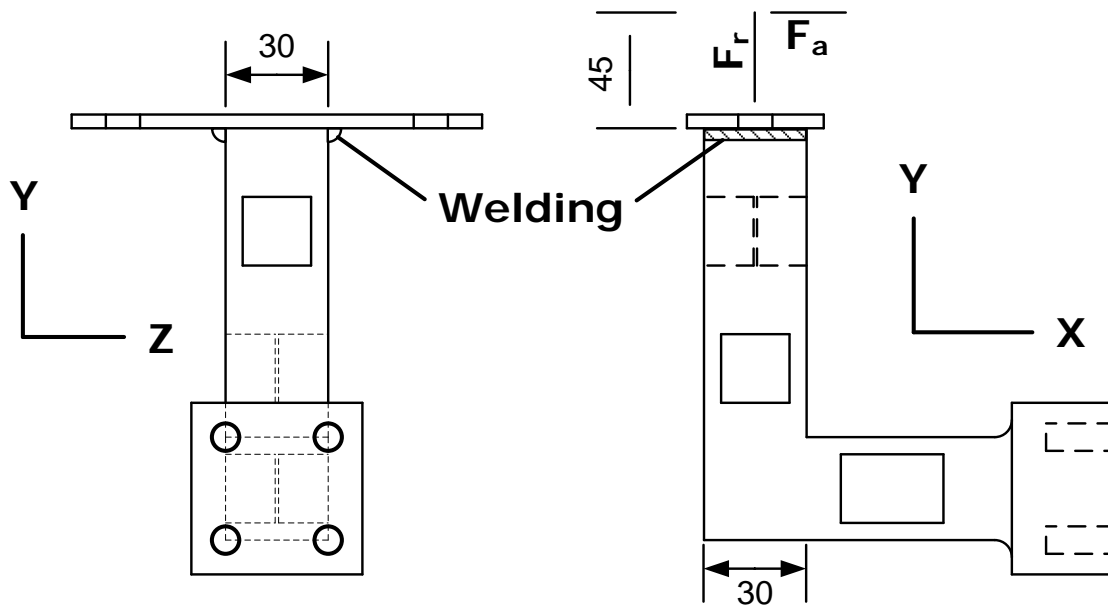


Figure 29: The convex welding location on transducer.

The throat area can be calculated:

$$A_s = l_e \cdot a_e = 2 \cdot 18 \text{ mm} \cdot 6 \text{ mm} = 216 \text{ mm}^2 \quad (4-72)$$

Where:

A_s : The throat area to the both sides [mm^2]. (10)

l_e : The length of throat area $l_e = l - 2a$ [mm].

a_e : The width of throat area $a_e = 0.75 \cdot (a + 2)$ [mm]. (See Figure 30)

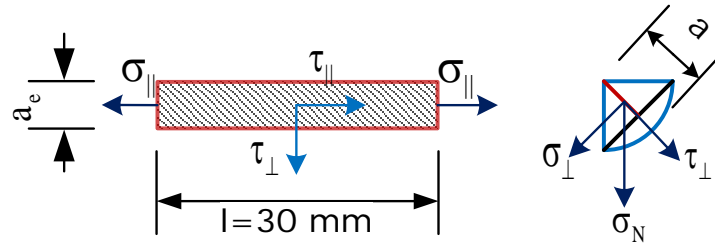


Figure 30: The illustration of the welding throat area.

The throat area's normal stress can calculate such:

$$\sigma_{\perp} = \tau_{\perp} = \frac{\sigma_N + \sigma_b}{\sqrt{2}} = \frac{1}{\sqrt{2}} \cdot \left(\frac{F_r}{A_s} + \frac{M_b}{2 \cdot W} \right) = \frac{1}{\sqrt{2}} \cdot \left(\frac{1800 \text{ N}}{216 \text{ mm}^2} + \frac{720 \text{ N} \cdot 45 \text{ mm} \cdot 6}{2 \cdot 6 \text{ mm} \cdot (18 \text{ mm})^2} \right) = 41.2 \text{ MPa} \quad (4-73)$$

Where:

σ_{\perp} : The throat area's normal stress [MPa].

τ_{\perp} : The throat area's normal shear stress [MPa]. (10)

σ_N : The normal stress [MPa].

σ_b : The bending stress [MPa].

M_b : The bending moment [Nmm].

W : The section modulus $W = \frac{1}{6} \cdot a_e \cdot l_e^2$ [mm³].

F_r : The radial or normal force [N]. (See Figure 29)

But the throat area's parallel shear stress calculates:

$$\tau_{\parallel} = \frac{F_a}{A_s} = \frac{720 \text{ N}}{216 \text{ mm}^2} = 3.3 \text{ MPa} \quad (4-74)$$

Where:

τ_{\parallel} : The throat area's parallel shear stress [MPa]. (10)

F_a : The axial force [N].

The static equivalent stress is then:

$$\sigma_{ae} = \sqrt{\sigma_{\perp}^2 + 3 \cdot \tau_{\perp}^2 + 3 \cdot \tau_{\parallel}^2} = \sqrt{(41.2)^2 + 3 \cdot (41.2)^2 + 3 \cdot (3.3)^2} = 82.6 \text{ MPa} \quad (4-75)$$

The obtained equivalent stress with material yield strength is checked by:

$$\eta = \frac{R_{p0.2}}{\sigma_{ae}} = \frac{380 \text{ MPa}}{82.6 \text{ MPa}} = 4.6 \quad (4-76)$$

Where:

η : The safety factor.

$R_{p0.2}$: The yield strength [MPa].

The wilding's safety factor $\eta = 4.6$, is OK.

4.10. The Spring:

As shown in the Figure 27 there is a helical compression spring between the bushing which attached to the thrust bearing and the axial-bolt. The spring will be useful during the calibration of the axial load to run the CBM test. The spring's requirement data is sets up as follows:

The inner diameter is $D_i = 16$ mm.

The demand compression $\delta = L_o - L_n = 10$ mm.

The force $S = 720$ N.

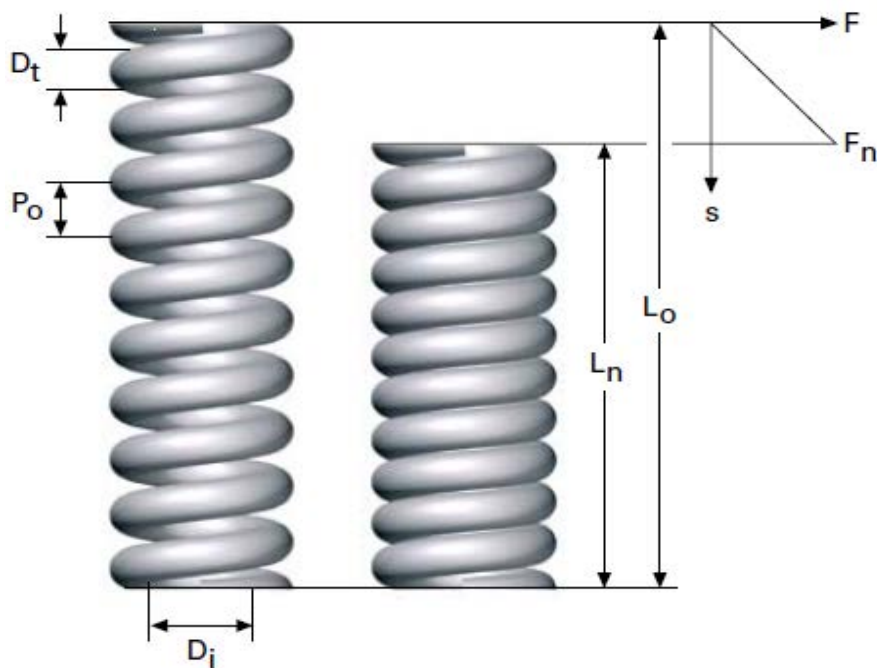


Figure 31: The compression spring drawing from Lesjøfors AS.


The spring was selected from Lesjøfors AS catalogue. (25 pp. 44 - 45)

A compression spring **SF-TFX Art. No. 2747.**

5. THE DYNAMIC MODEL OF THE SHAFT

This chapter will present the simulation of the dynamic model of the shaft and the main focus is what the test bearing will be experiencing during the operation in purpose to improve the knowledge in the dynamic model analysis. The dynamic model analysis is carried out in SimulationX 3.3 program with a simplified shaft model.

5.1. The Dynamic Model:

The test-rig's shaft has been presented early in this report (see sub-chapter 3.2). The shaft model was built in SimulationX by verifying the interest criteria such that the model includes just the part of shaft between the reaction-forces (between point A and B in Figure 3). The modeled shaft is divided to the ten Cylinder  elements with $L = 50$ mm in length except for the yellow ring has $L_R = 25$ mm, the blue elements' which have diameter $D_B = 35$ mm, the green and orange elements' diameter $D_{G,O} = 40$ mm and the yellow ring has inner diameter $d_Y = 40$ mm and outer diameter $D_Y = 46$ mm.

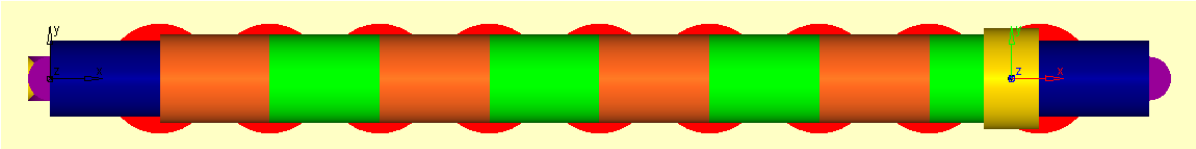


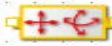


Figure 32: The modeled shaft in SimulationX.

Between every two elements placed three Revolute Joints  element type from MBS Mechanics tool box for every direction X, Y, & Z each and one Spring-Damper  (the red circles in the figure above represent the spring-damper in SimulationX). The damper values considered to be low and same value in all directions but the spring stiffness coefficients are calculated based on the element's diameter and torsion or bending stiffness. The torsion spring stiffness is applied in X direction where the shaft is rotating about X-axis. But the bending spring stiffness is applied in Y & Z directions. Constraint  element type from MBS Mechanics has been used in the other end of the modeled shaft and fixed in the **Translative Constraint** in Y & Z direction.

The spring bending-stiffness coefficient can be calculated by the supervisor's handed out equation:

$$k_B = \frac{2 \cdot E \cdot I}{L} \quad (5-1)$$

Where:

k_B : The spring bending-stiffness coefficient [Nm/rad].

E: The material's young's modulus [MPa].

I: The 2nd moment of inertia $I = \frac{\pi \cdot D^4}{64}$ [mm⁴], D is the element's diameter [mm].

L: The element's length [mm].

The spring torsion-stiffness coefficient can be computed by supervisor handed out equation:

$$k_T = \frac{2 \cdot G \cdot I_P}{L} \quad (5-2)$$

Where:

k_T : The spring torsion-stiffness coefficient [Nm/rad].

G: The material's shear modulus $G = \frac{E}{2(1+\nu)}$ [MPa], ν is the material's Poisson ratio.

I_P : The polar 2nd moment of inertia [mm⁴], $I_P = \frac{\pi \cdot D^4}{32}$.

The equivalent spring stiffness coefficient which the springs are in series can calculate:

$$\frac{1}{k_{eq}} = \frac{1}{k_1} + \frac{1}{k_2} \rightarrow k_{eq} = \frac{k_1 \cdot k_2}{k_1 + k_2} \quad (5-3)$$

Where:

k_{eq} : The equivalent spring stiffness coefficient [Nm/rad].

k_1 : The spring stiffness coefficient for one element [Nm/rad].

k_2 : The spring stiffness coefficient for the next element [Nm/rad].

The calculation of the spring stiffness carried out one time for the bending and the other time for torsion, the results will be presented in the following tables.

Table 7: The elements and material data.

L [mm]	ν	E [MPa]	G[MPa]
50	0.3	210,000	80770


Table 8: The profile calculation.

D [mm]	I [mm ⁴]	I _p [mm ⁴]
35	73661.8	147323.5
40	125663.7	251327.4

Table 9: The spring stiffness coefficients results.

Spring stiffness	k_{35} [Nm/rad]	k_{40} [Nm/rad]	$k_{eq,40-40}$ [Nm/rad]	$k_{eq,40-35}$ [Nm/rad]
Bending	618,759	1,055,575	527,788	390,093
Torsion	475,968	811,981	25,374	300,072

The shaft's model is exposed for radial load in the simulation but the axial load is ignored.

The radial load is applied by ***Spherical Body***  element type from MBS Mechanics tool box with radius $r = 1.5$ mm and mass $m = 200$ kg in value in the center of the local coordinate of yellow ring (see Figure 32) which represent the inner ring of the Needle-bearing.

5.2. The Angle of Deflection:

The angle of deflection is one of the interested criteria to compare the modeled shaft in SimulationX with the designed shaft. The angle of deflection of the designed shaft was calculated at the points A & B and the shaft was assumed as uniform with diameter $D = 35$ mm.

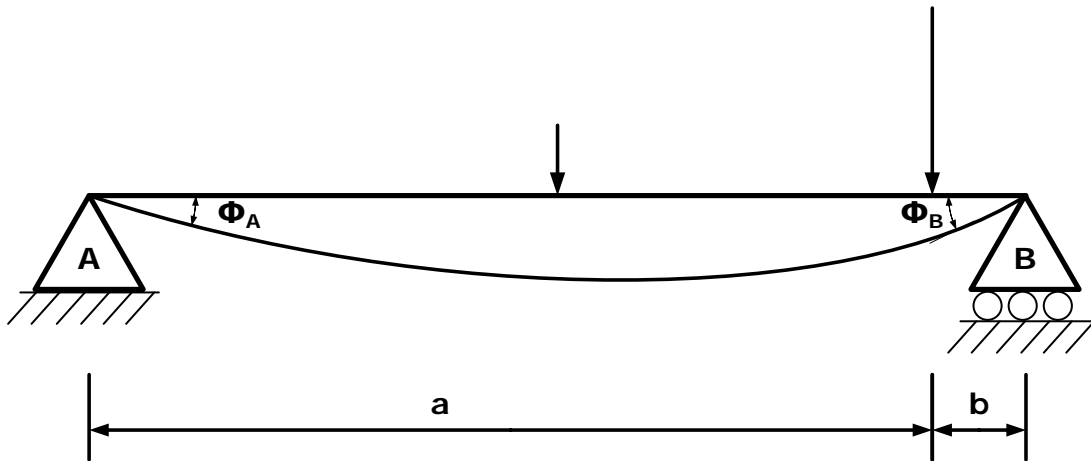


Figure 33: Illustration of the shaft and angle of deflection.

First the angle of deflection which caused by the shaft own gravity forces:

$$\phi_{A,q} = \phi_{B,q} = \frac{qL^3}{24EI} = \frac{(\rho g A)L^3}{24EI} = \frac{7.85 \cdot 10^{-6} \left(\frac{\text{kg}}{\text{mm}^3}\right) \cdot 9.81 \left(\frac{\text{m}}{\text{s}^2}\right) \cdot 1257 \text{mm}^2 \cdot 500^3 \text{mm}^3}{24 \cdot 210000 \text{MPa} \cdot 73662 \text{mm}^4} = 0.0018^\circ \text{ (5-4)}$$

Where:

$\phi_{A,q}$ & $\phi_{B,q}$: The angle of deflection caused at constraint A & B [°]. (21 p. 531)

q : The load distribution per length [N/m], $q = \rho g A$.

ρ : The steel mass density [kg/mm^3].

g : The gravity acceleration [m/s^2].

A : The cross section area [mm^2], $A = \pi r^2$.

r : The cylindrical shaft radius [mm].

L : The length of uniform shaft or beam [mm].

E : The Young's modulus [MPa].

I : The 2nd moment of inertia [mm^4], $I = \frac{\pi r^4}{4}$.

Next the angle of deflection which is caused by the radial load:

$$\begin{cases} \phi_{A,F} = \frac{Fab(a+2b)}{6LEI} = \frac{1800N \cdot 450mm \cdot 50mm \cdot (450mm + 2 \cdot 50mm)}{6 \cdot 500mm \cdot 210000MPa \cdot 73662mm^4} = 0.03^\circ \\ \phi_{B,F} = \frac{Fab(2a+b)}{6LEI} = \frac{1800N \cdot 450mm \cdot 50mm \cdot (2 \cdot 450mm + 50mm)}{6 \cdot 500mm \cdot 210000MPa \cdot 73662mm^4} = 0.051^\circ \end{cases} \quad (5-5)$$

Where:

$\phi_{A,F}$ & $\phi_{B,F}$: The angle of deflection caused at constraint A & B [°]. (21 p. 531)

F: The radial load [N].

a: The distance between constraint A to the radial force [mm].

b: The distance between constraint B to the radial force [mm].

Then the total angle of deflection at the constraint A & B is:

$$\begin{aligned} \phi_{totA} &= \phi_{A,q} + \phi_{A,F} = 0.0018^\circ + 0.03^\circ = 0.031^\circ \\ \phi_{totB} &= \phi_{B,q} + \phi_{B,F} = 0.0018^\circ + 0.052^\circ = 0.053^\circ \end{aligned} \quad (5-6)$$

Where:

$\phi_{tot,A}$: The total angle of deflection at constraint A [°].

$\phi_{tot,B}$: The total angle of deflection at constraint B [°].

The angle of deflection results from SimulationX is illustrated in following figures:

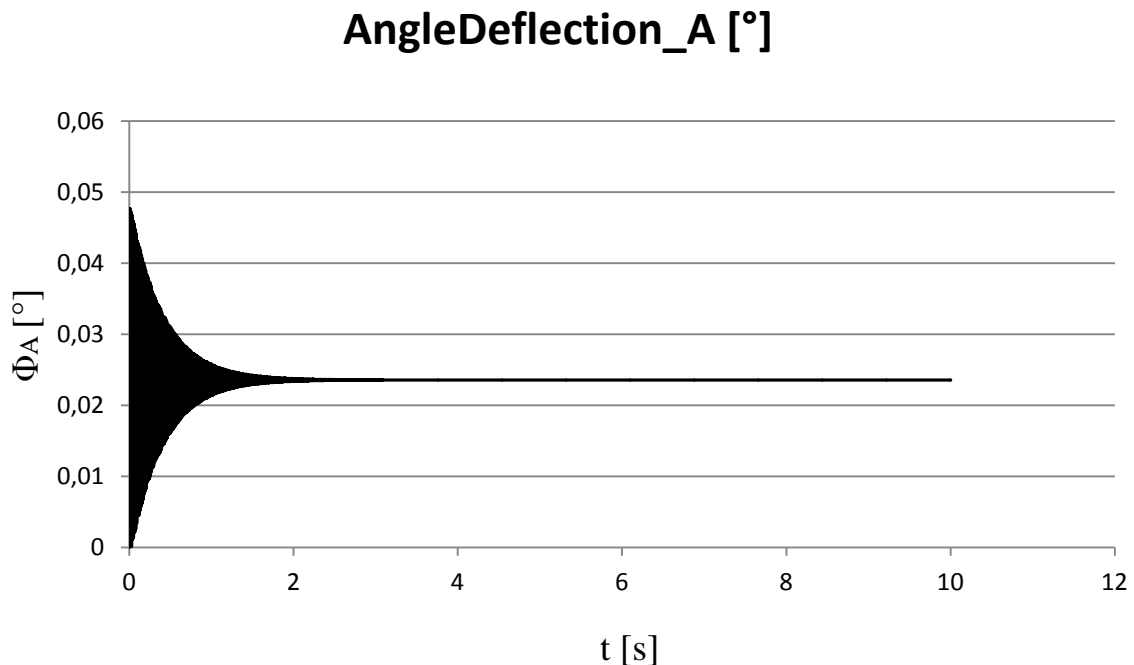


Figure 34: the angle of deflection at constraint A.

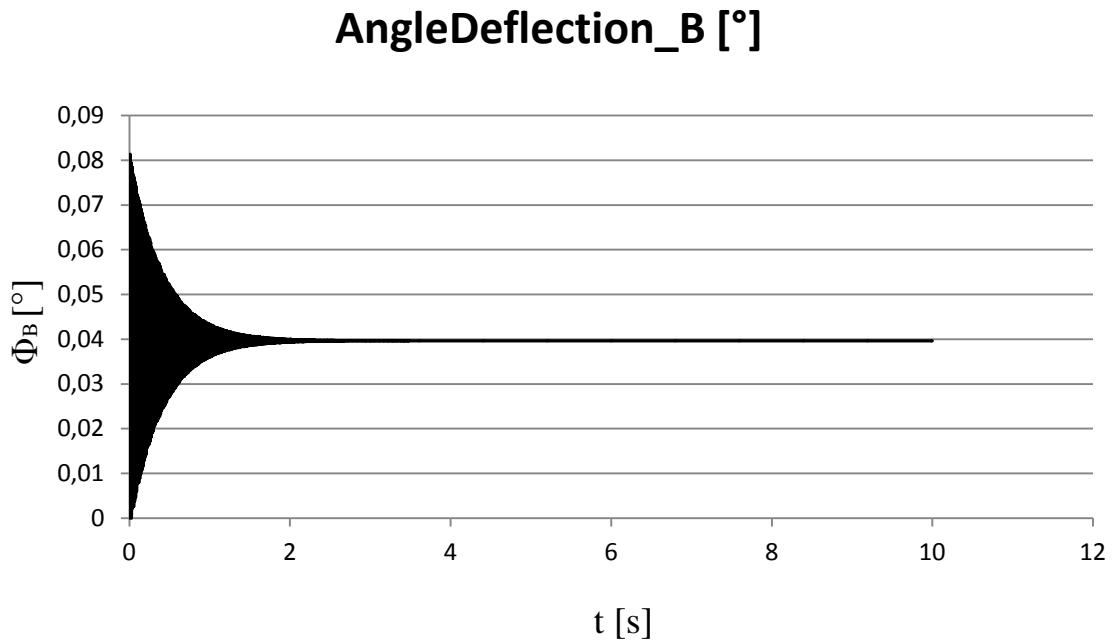




Figure 35: The angle of deflection at constraint B.

In comparison of the designed shaft with the dynamic model, there is some deviation. The deviation could be caused firstly by the assumption made earlier where the shaft is uniform. Secondly the location of the simulated angle of deflection is in the center of the cylinder element which means 25 mm from the constraint. Therefore the model is acceptable.

5.3. The Critical Speed

The next criterion is to investigate the critical speed of the dynamic model. Add in to the model **Preset**  element type from Rotational Mechanics tool box which is connected to the shaft model by an **Actuated Revolute Joint**  element type within driving flange CtrR2 connector, and apply an angular speed as a function of time t with initial value $\omega = 3000 \text{ rpm}$ and with relatively smooth slope increasing the speed up to critical speed area. The observed critical speed is about $\omega_{cr} = 5200 \text{ rpm}$.

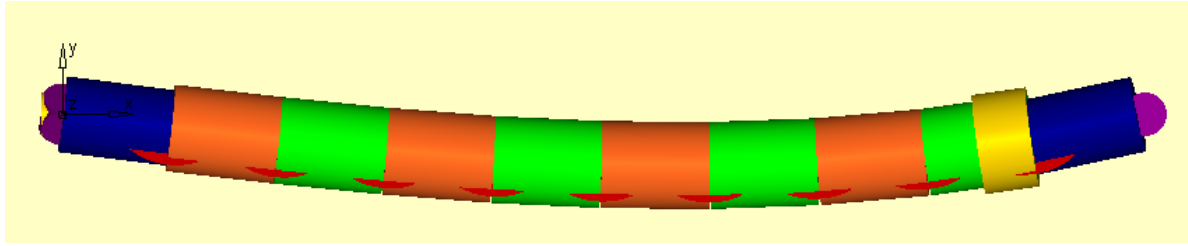


Figure 36: The illustration of the shaft's bending occurs because of the critical speed.

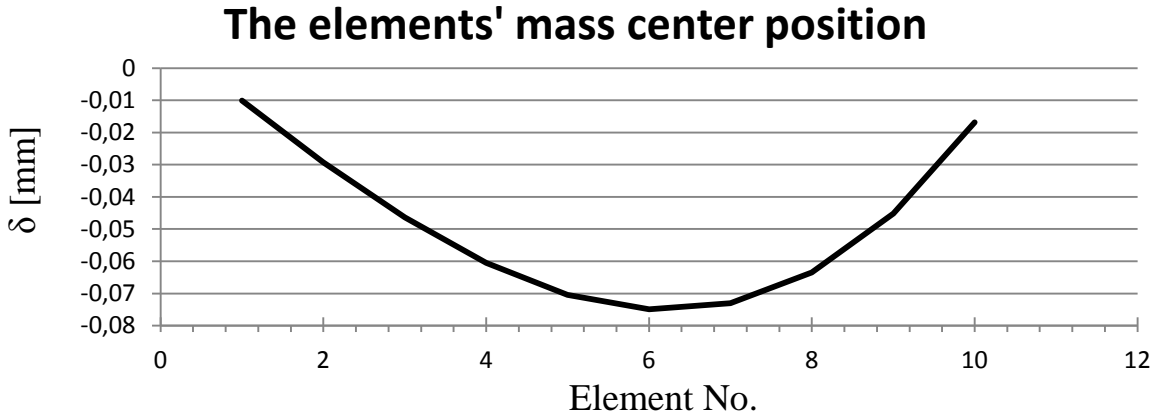
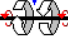


Figure 37: The deflection of the shaft at the critical speed.

The calculated natural frequency for the designed shaft is $\omega_N = 3624 \text{ rpm}$ and the simulated of the dynamic model is 5200 rpm. The deviation is caused by the assumption which has been made in the calculation as the uniform shaft.

5.4. The Reaction Force at Test-bearing

The reaction forces at constraint which is representing the test-bearing in the designed test-rig, can be analyzed by the dynamic model to improve the knowledge in purpose to establish CBM for rotating machinery. The motion was applied by External Torque  element type from Rotational Mechanics tool box with fixed angular speed $\omega = 3000 \text{ rpm}$ about X direction. (See Appendix C - Figure 56)

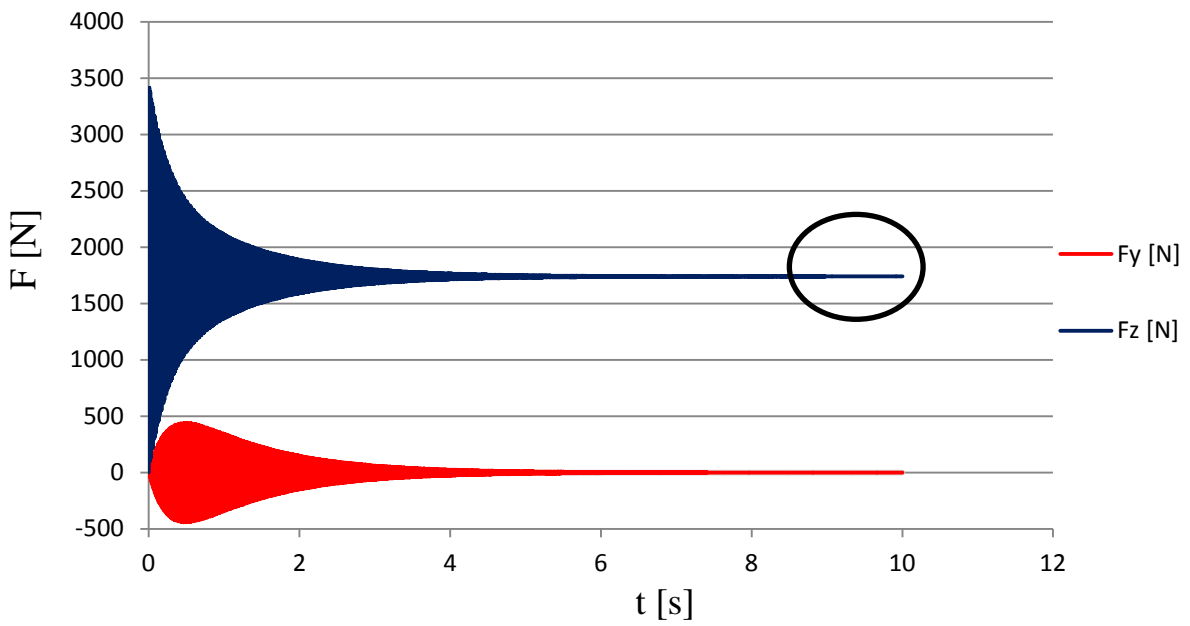


Figure 38: The kinematic analysis results at Constraint (B).

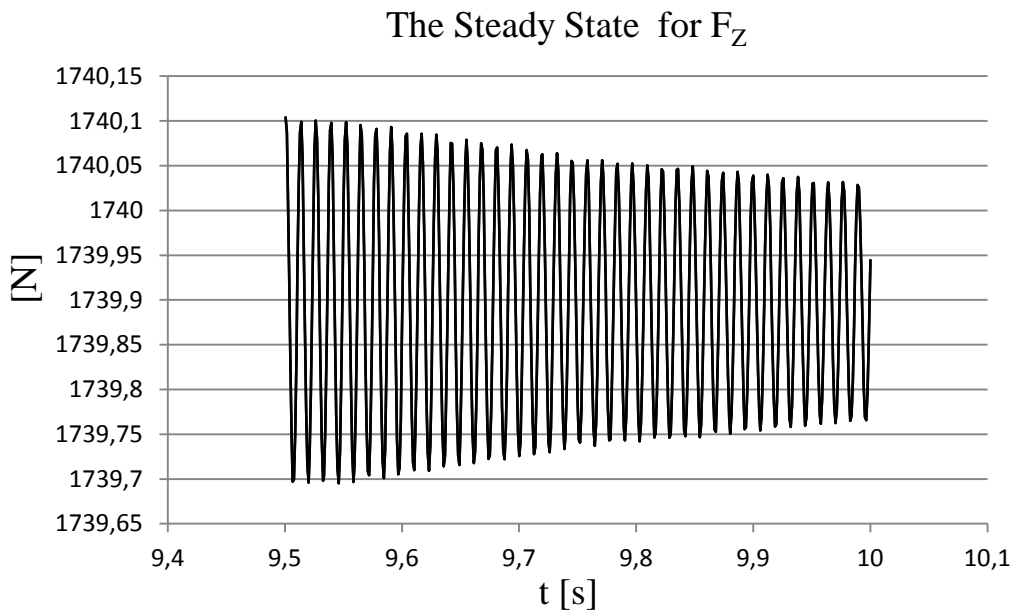


Figure 39: The steady state results of the kinematic analysis at Constraint (B).

The Dynamic model simulation shows that the reaction forces F_Y & F_Z reach the steady state value about $t = 5s$ with $F_Z = 1739.9$ N where the calculated reaction force was $B_Y = 1786$ N.

6. THE LABVIEW

Since this project, is about performing destructive test to estimate the bearing's effective lifetime, and to shorten the test duration to be able to run the test several times; so it requires to design an automatic Switch Off program to prevent further damage to the entire test facility when nobody monitoring the test equipment. The figures below shows an automatic switch off control panel of the electric actuator which is programmed in LabView program.

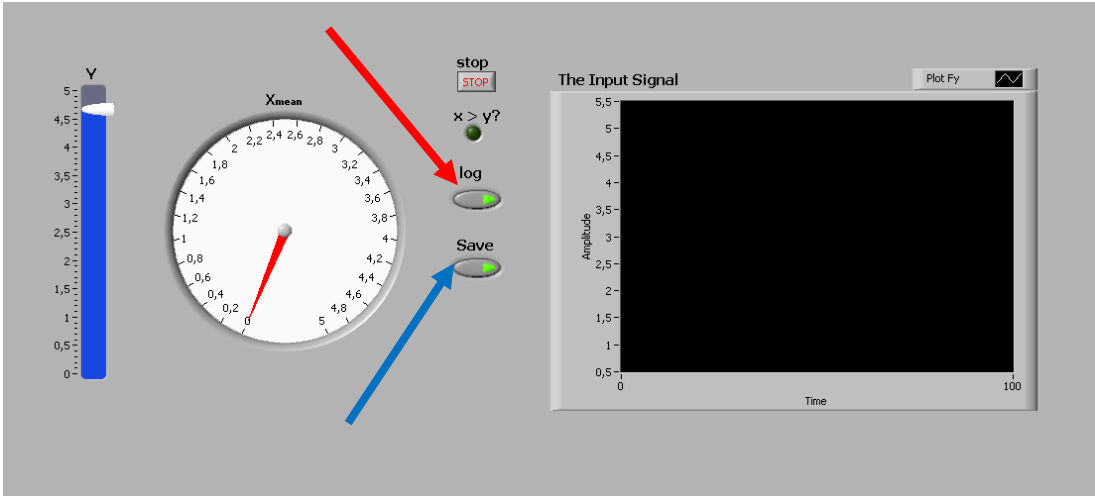


Figure 40: The illustration of an automatic switch off control panel in LabView.

The mechanism of the program works in this way, the program read the strain gages' signals as Input and it monitors the signals developments until the signals reach a specific level which is an indication of bearing failure. The specific level has been already defined in the program. So the DC motor will be switched off automatically. Further on when the **log** bottom (red arrow in Figure 40) is ON during the test it will note the strain gages' signals with resolution 100 samples per second and store them in shift register (temporary) until the **save** bottom (blue arrow in Figure 40) is clicked then all the data will be stored or saved on the C disk of the PC for further analysis and usage. (See Appendix A)

The communication between the Switch Off program and the sensors (strain gages) are taking place by an I/O card NI USB-6008 model and HEXFET power MOSFET (IRF3415) circuit. (See Figure 41)

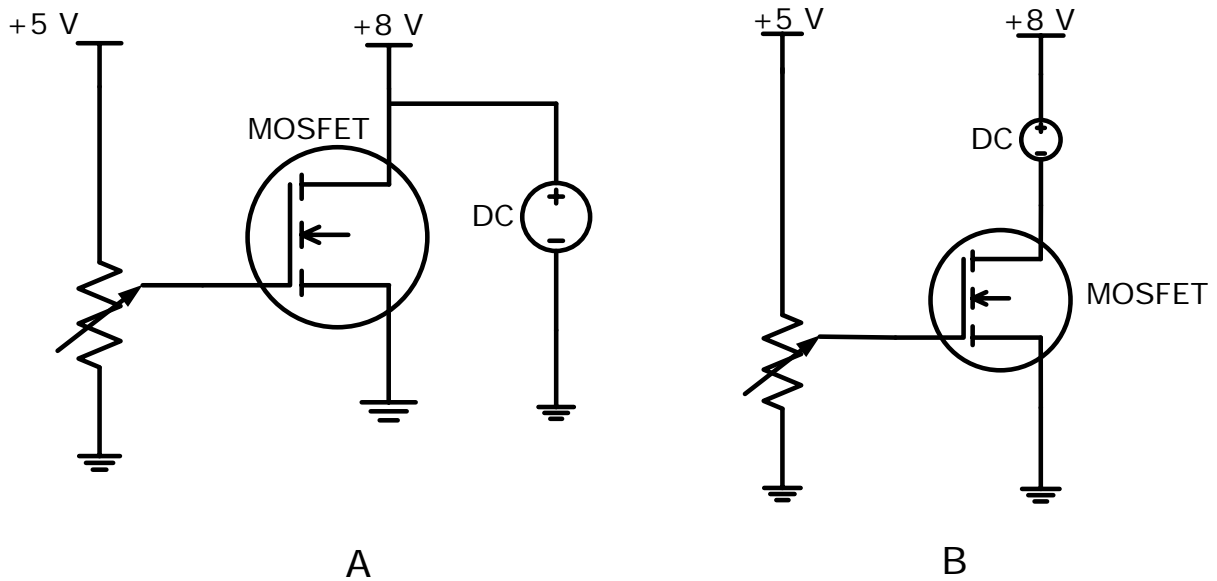


Figure 41: The three ports MOSFET circuit. A) The built circuit, B) The correct circuit.

The Switch Off program has been tested to check the functionality. The results were satisfying the demand such monitoring, collecting and storing of data (Input signal) and automatic disconnecting of DC motor. During the test, the MOSFET circuit **A** has been used. In circuit **A** the DC motor is connected parallel which can lead to continuous running of the DC motor. But the reason that the circuit **A** worked properly was because of the power supplier. The power supplier was not powerful enough. But in the MOSFET circuit **B**, the DC motor is in series, and the problem is solved.

7. THE TEST PROCEDURE

In purpose to run the CBM test, there are some steps which have to be taken into consideration, so as to obtain acceptable and reliable results. The recommended steps are as the following:

- Calibrating the strain gages which attached to transducer and this step is necessary just for 1st time up running the test. To calibrate the strain gages, the radial and axial load have to be removed and then set the input signals from the strain gages (transducer) to zero.
- Connecting the DC motor and the strain gages signals to the DC motor Switch-OFF control program and testing the functioning of it. (See Chapter 6)
- Assure the **log** bottom is clicked on during the test otherwise it will be no access to the required information (strain gages' signals) of the test. (See Figure 40)
- Clicking the **save** bottom (in LabView) at the end of the every test which will be saved automatically in the C hard disk. (See Figure 40)
- Taking good care and storing of the destroyed bearing when is being removed from its location, to make it possible for damage investigation and analysis. And the new test-bearing does not require any lubrication unless the goal is to perform the test with new specifications.
- Adjusting the reference signal in the LabView program based on the analysis of the stored data and the damaged bearing's disclosure to improve the CBM prediction.
- To be aware of that to modify the monitoring technique if it is necessary in purpose to gain better result (CBM). The monitoring technique can be modified by including different types of sensors (e.g. accelerometer, infrared heat detector camera, X-ray scanner and etc).

8. FURTHER WORK

The effort have been done during this project and the time have been spent, let me realize that the test rig can be modified even better if some changes take place. Among the other recommendations:

- Replace the load mechanism per today design with hydraulic actuators where the benefits are:
 1. To drop the lifting of the heavy steel blocks during the setup of the test-rig, and the replacement of the test-bearing when the failure occurs.
 2. To simplify the work when vary loads altitude is required.
 3. To be able to apply vary loads altitude during the test (by increasing or decreasing the load).

- Adding different type of sensors to the system to compare the most effective type of sensors according to the applications and the environment (e.g. Bearing, shaft, gear or offshore, onshore, airspace etc).
- To design a new program for the electrical actuator where to be able for applying vary speed and switch ON/OFF during the test in purpose to investigate the transient effect on the components life time, and nevertheless replacing the electrical motor with suitable one.
- Developing (programming) of dynamic model due to Shaft, Bearing and shaft-bearing for further analysis and investigation to improve the knowledge.

9. THE CONCLUSION

The goal of this thesis was initially to fulfill the design and building of nominated concept from the early stages of the project, and establishing the CBM for rotating machinery, it became clear however that, the building of test facility was beyond the scope of this master thesis. The project became focused on fulfillment of the design, calculation and dynamic model analysis of the rotating shaft. The results that have been achieved are highly relevant and enable the advancement of further works in the area of CBM for rotating machinery.

To compliment the design and calculation of the mechanical component were carried out, based on the Bachelor and Master Mechatronic course materials or the producer's own methods, data and formulas. The missing information has been covered by a conservative assumption or supervisors' guidance. The engineering drawings of the designed components were done. The static FEM analysis of the transducer due to investigation of the equivalent stresses level was done as well with satisfying results.

The dynamic model of the simplified shaft reveals what the test-bearing is experiencing during the operation especially at the transient part of the simulation. The equivalent load value can be doubled which means the operation sequence affects the bearing's lifetime.

10. REFERENCES

1. **Arvallo, Agustin Vasquez.** *Condition-Based Maintenance of Actuator Systems using a model-based approach.* [ed.] B.S., M.S. Agustin Vasquez Arvallo. Austin : University of Texas, 2000. p. 1.
2. **R. Keith Mobley, Lindey R. Higgins and Darrin J. Wikoff.** *Maintenance Engineering Handbook.* 7th. Edition. New York : McGraw Hill, 2008. p. 37.
3. **Marc P. Gaguzis, MAJ.** *Effectiveness Of Condition Based Maintenance In Army.* West Point : United States Military Academy, 1998. p. 2. A thesis presented to the Faculty of the U. S. Army Command and General Staff College in partial fulfillment of the requirements for MAster of Military Art and science.
4. **Mobley, Keith R.** *AN INTRODUCTION TO PREDICTIVE MAINTENANCE.* [ed.] Elsevier Science. s.l. : Second Edition, Copyright © 2002. ISBN: 0-7506-7531-4.
5. **Smith, Dr. David J.** *RELIABILITY, MAINTENABILITY AND RISK.* 6. Edition. s.l. : Butterworth Heinemann Ltd. Vol. 2001.
6. *Implelmentation Strategies and Tools for Condition Based Maintenance at Nuclear Power Plants.* International Atomic Energy Agency. Vienna : s.n. pp. 14, 15.
7. **Dileo, Mike, Manker, Charles og Cadick, John.** *Condition Based Maintenance.* s.l. : P. E., 1999.
8. **Djokoto, Sylvester S. og Mashat, Hussein A.** *Condition Based Maintenance on Rotating Systems.* Mechatronic Department, UiA. Grimstad : s.n., 2009. Cours Work.
9. The steel material data. [Internett] 2010. <http://www.mesteel.com/info/german.htm>.
10. **Robbersmyr, Kjell Gunnar.** *Maskin Deler.* [Compendium] Trondheim : s.n., 1996.
11. The Roller Bearing. [Internett] SKF.com.
<http://www.skf.com/portal/skf/home/products?maincatalogue=1&lang=en&newlink=1>.
12. The Calculation of Roller Bearing. [Internett] SKF.com.
<http://www.skf.com/skf/productcatalogue/jsp/calculation/calculationIndex.jsp?&maincatalogue=1&lang=en>.
13. The Cylindrical Bearing. [Internett] SKF.com.
<http://www.skf.com/skf/productcatalogue/Forwarder?action=PPP&lang=en&imperial=false&>windowName=null&perfid=141024&prodid=1410241007>.

14. The Ball Bearing Life. [Internett] SKF.com.
http://www.skf.com/portal/skf/home/products?lang=en&maincatalogue=1&newlink=1_0_21.
15. The Equivalent Dynamic Bearing Load (Ball Bearing). [Internett] SKF.com.
http://www.skf.com/portal/skf/home/products?maincatalogue=1&lang=en&newlink=1_1_14.
16. The Ball Bearing. [Internett] SKF.com.
<http://www.skf.com/skf/productcatalogue/Forwarder?action=PPP&lang=en&imperial=false&windowName=null&perfid=101002&prodid=1010021804>.
17. Units Conversion Factors For Bearing Life. [Internett] SKF.com.
http://www.skf.com/skf/productcatalogue/jsp/viewers/tableViewer.jsp?tableName=1_0_t40.tab&maincatalogue=1&lang=en.
18. The Cylindrical Thrust Bearing. [Internett] SKF.com.
<http://www.skf.com/skf/productcatalogue/Forwarder?action=PPP&lang=en&imperial=false&windowName=null&perfid=173001&prodid=173001104>.
19. The frictional momentum - SKF.com. [Internett] Roller Bearing, Bearing house, Coupling, etc.
http://www.skf.com/portal/skf/home/products?maincatalogue=1&lang=en&newlink=1_0_36#
 .
20. Contant Coefficient of friction. [Internett] SKF.com.
http://www.skf.com/skf/productcatalogue/jsp/viewers/tableViewer.jsp?tableName=1_0_t6.tab&maincatalogue=1&lang=en.
21. **Irgens, Fridtjov.** *Fasthetslære*. 6. Edition. Trondheim : Tapir - Forlag, 1999. ISBN 82-519-1522-8.
22. **Hoffmann, Karl.** *An Introduction to Measurements using Strain Gages*. Darmstad : Hottinger Baldwin Messtechnik GmbH.
23. **Institutionen for hållfasthetslära KTH.** *Handbok och formelsamling i Hållfasthetslära*. s.l. : VETENSKAPM OCH KONST.
24. **Juvinall, Robert C. and Marshek, Kurt M.** *Fundamentals of MACHINE COMPONENT DESIGN*. 4. Edition. s.l. : John Wiley & Sons, 2006. p. 769. ISBN 0-471-74285-6.
25. **Lesjöfors.** Lesjöfors Springs & Pressings. [Online] http://www.lesjoforsab.com/teknisk-information/standard_stock_springs_catalogue_13_-_norwegian_id1104.pdf.
26. **Carvill, J.** *Mechanical Engineering's Data Handbook*. pp. 94, 95, 96,97, 93, 94.

27. **Harris, Tedric A. and Michael, Kotzalas N.** *Essential Concept of Bearing Technology (Roller Bearing Analysis)*. Fifth Edition.

28. The Needle Bearing. [Internett] SKF.com.

<http://www.skf.com/skf/productcatalogue/Forwarder?action=PPP&lang=en&imperial=false&windowName=null&perfid=146245&prodid=146245008>.

29. Press Fits For Solid Steel Shaft. [Internett] SKF.com.

http://www.skf.com/skf/productcatalogue/jsp/viewers/tableViewer.jsp?tableName=1_0_t26&maincatalogue=1&lang=en.

30. SNL Bearing House. [Internett] SKF.com.

http://www.skf.com/skf/productcatalogue/jsp/viewers/tableViewer.jsp?tableName=5_16_t12.tab&maincatalogue=1&lang=en.

31. **Lesjöfors.** Lesjöfors Springs & pressings. [Internett] Lesjöfors. <http://www.lesjofors.no/>.

32. **SKF.** SKF.com. [Internett]

<http://www.skf.com/skf/productcatalogue/Forwarder?action=PPP&lang=en&imperial=false&windowName=null&perfid=520190&prodid=5201900505>.

11. APPENDICES

Appendix A

The Switch OFF of electrical actuator program

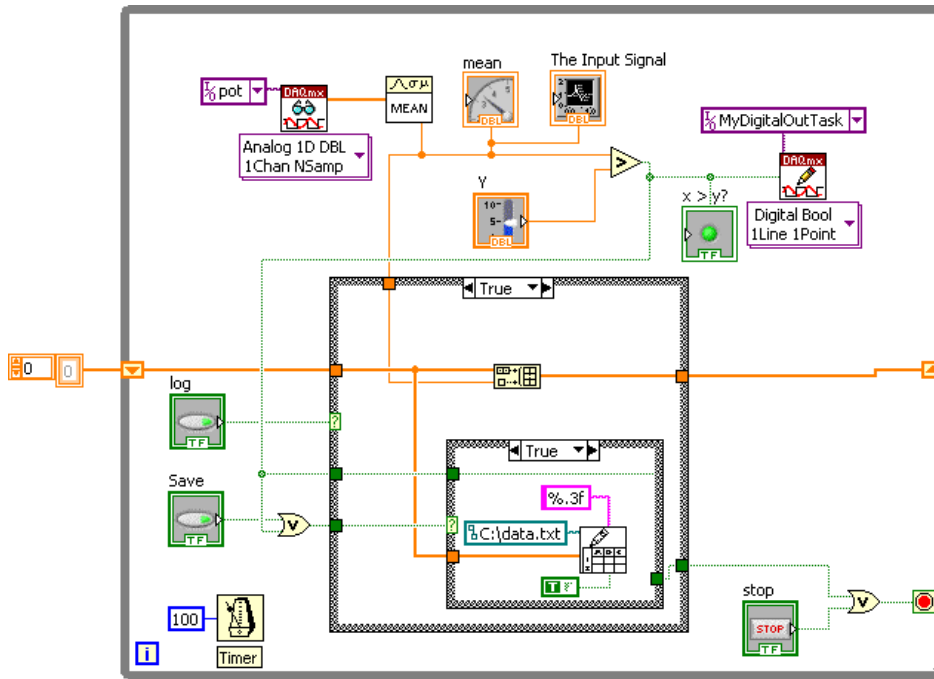


Figure 42: The block diagram of the motor Switch-OFF program with true condition in sub-loop.

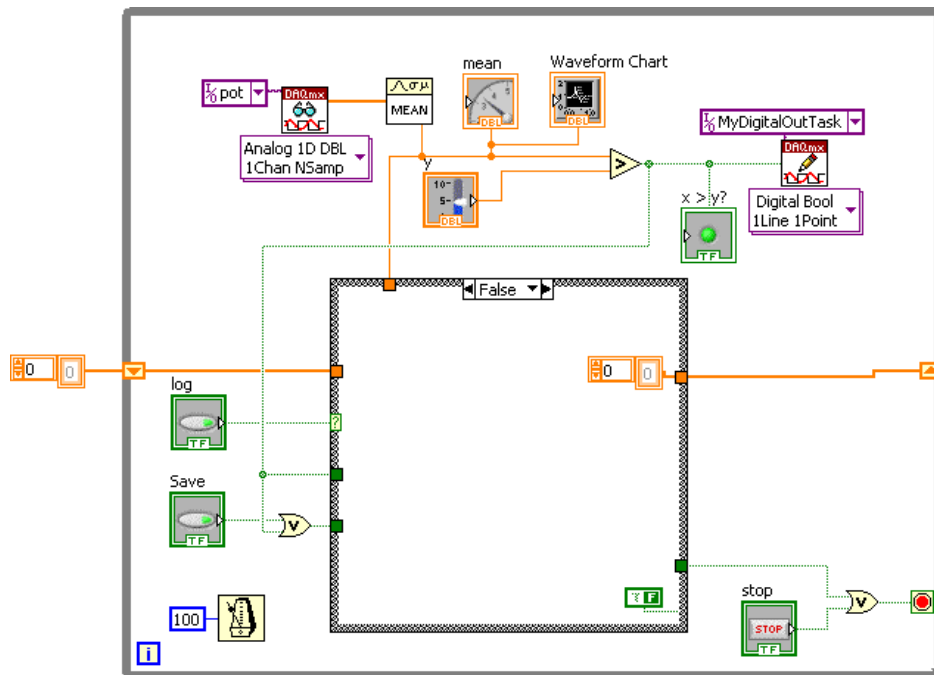


Figure 43: block diagram of the motor Switch-OFF program with false condition in sub-loop.

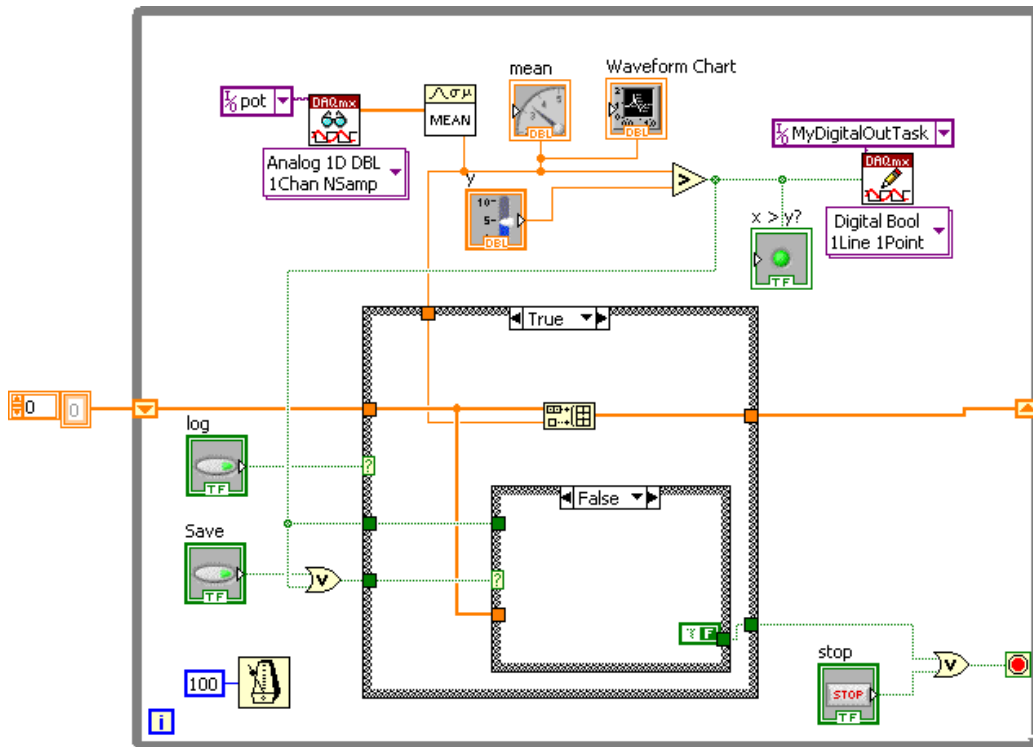


Figure 44: The block diagram with false condition in sub-sub-loop.

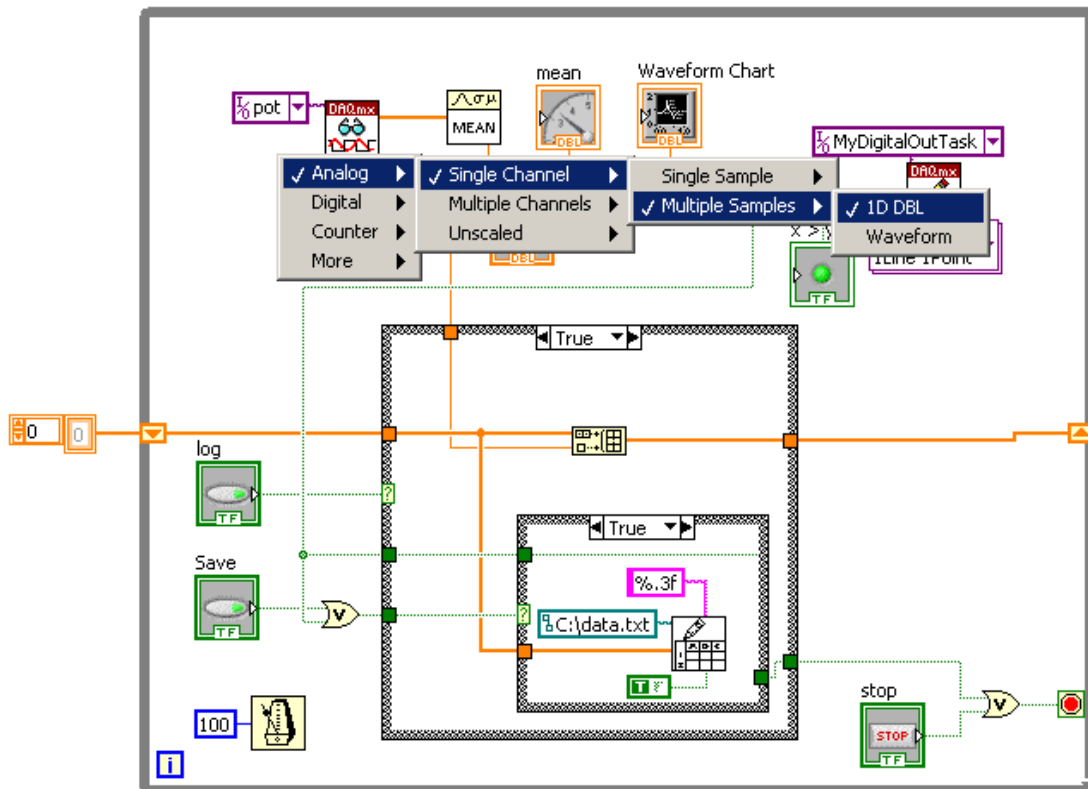


Figure 45: The setup of Input signal.

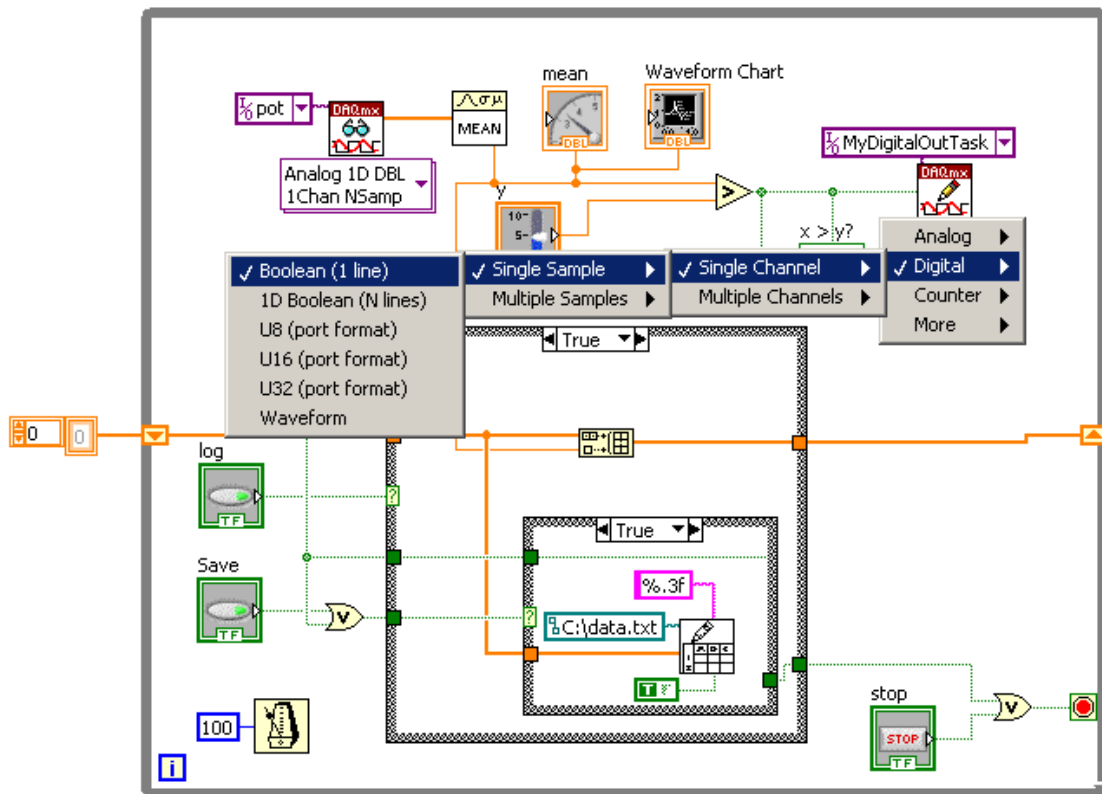


Figure 46: The setup of Output signal.

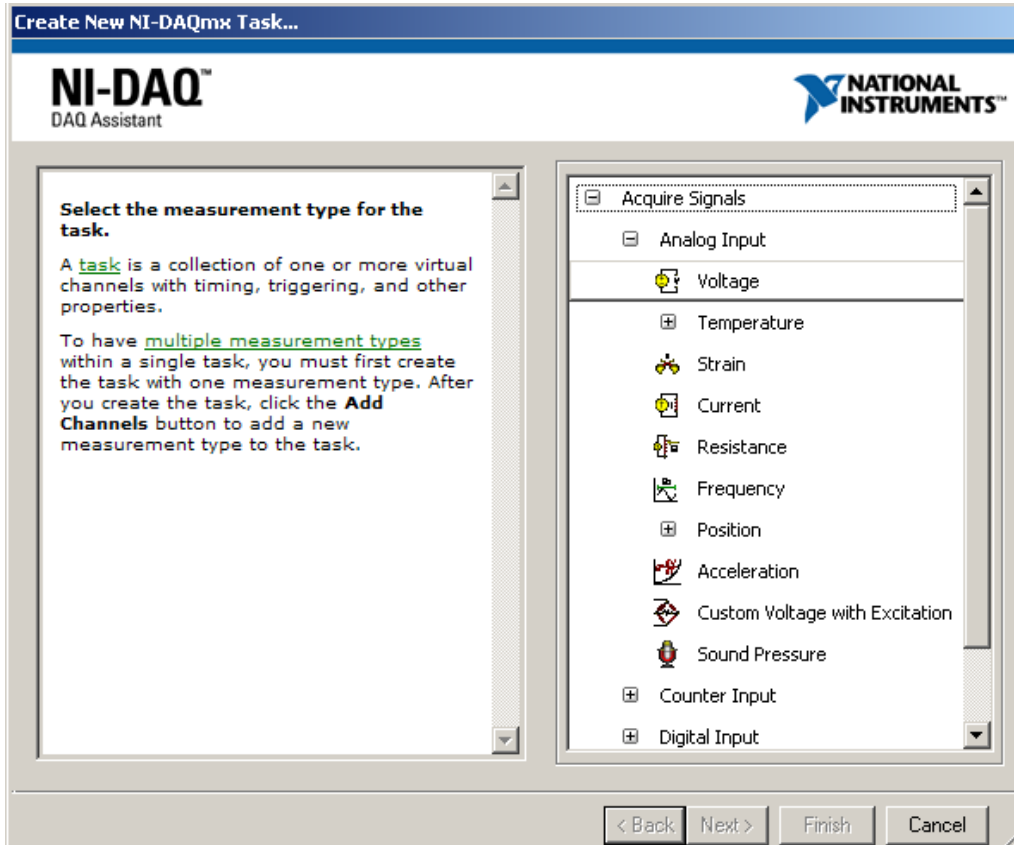


Figure 47: The acquire signal for Input.

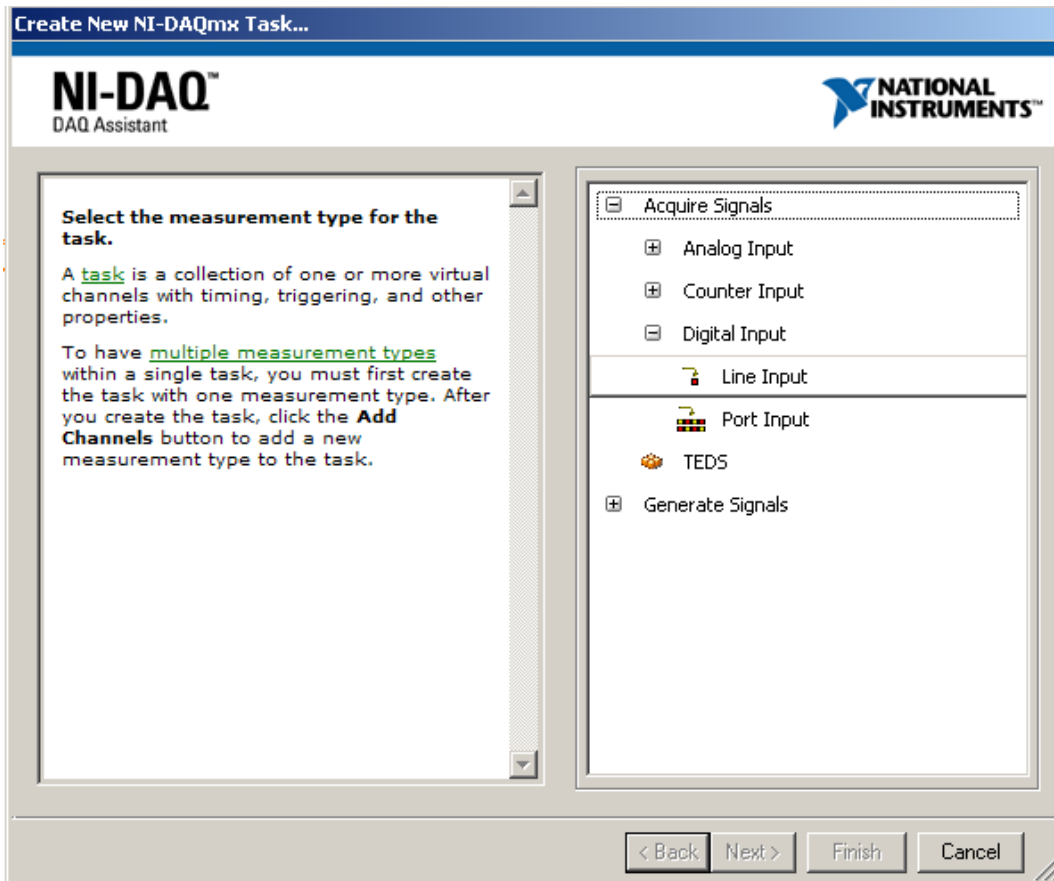


Figure 48: The acquire signal for Output.

Appendix B

The FEM analysis of the transducer

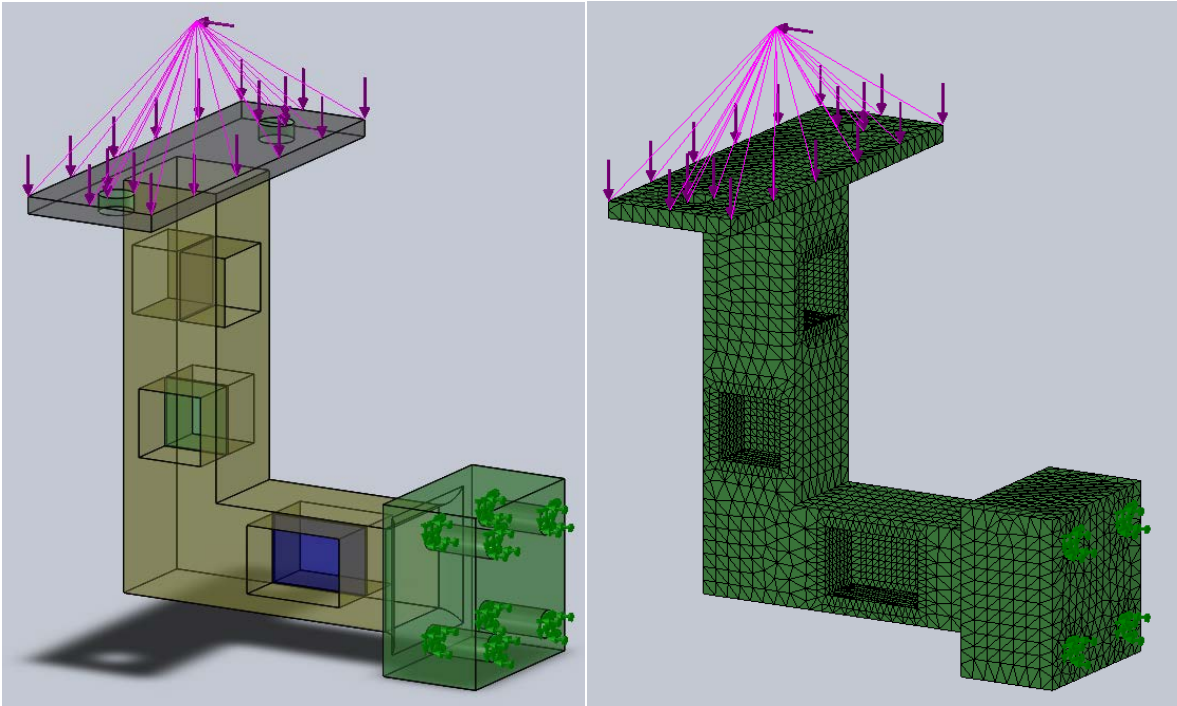


Figure 49: The Transducer views in Simulation, with Loads and constraints (left), plus mesh (right).

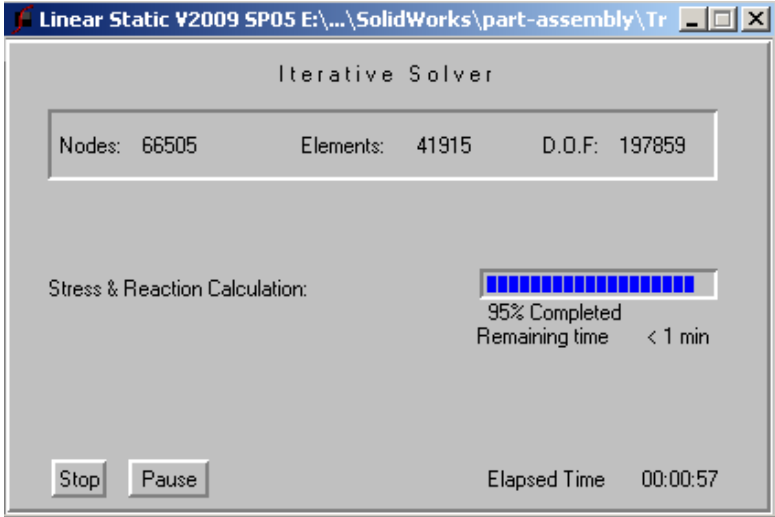


Figure 50: The generated nodes elements and degrees of freedom in Simulation due to Transducer's FEA.

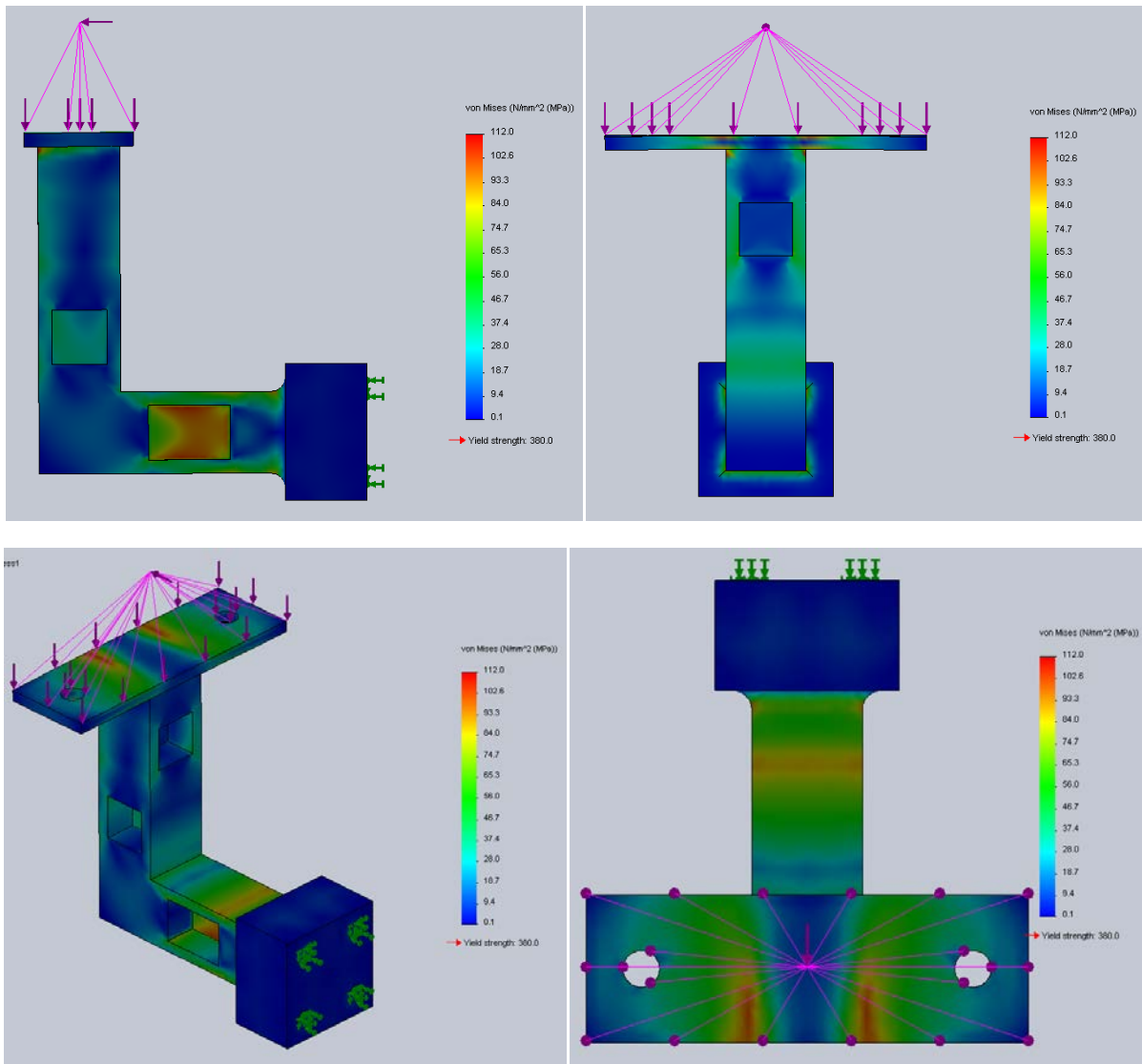


Figure 51: Different angles of view of Transducer with the simulated stresses in Simulation.

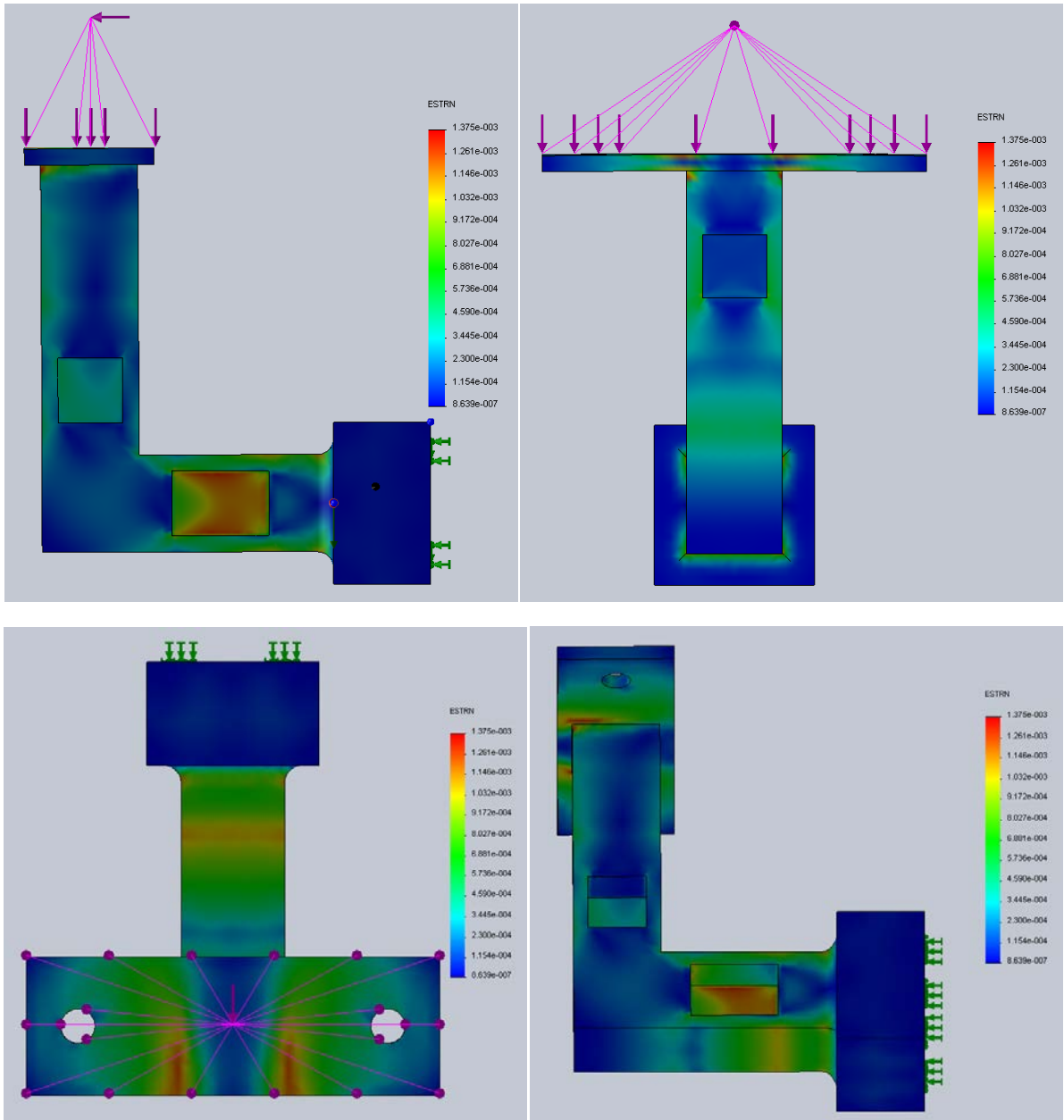


Figure 52: Different angles of view of Transducer with the simulated strain in Simulation.

Appendix C

The dynamic model of the shaft

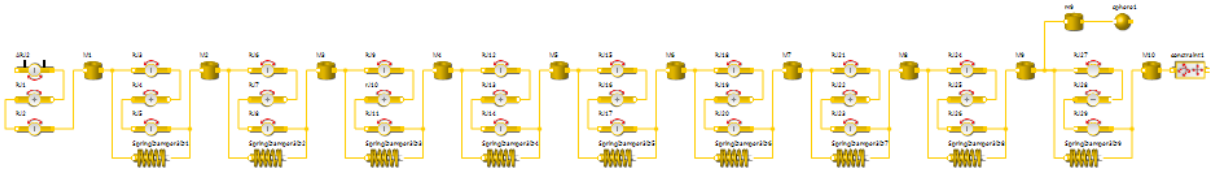


Figure 53: The setup of dynamic model due to angle deflection criterion.

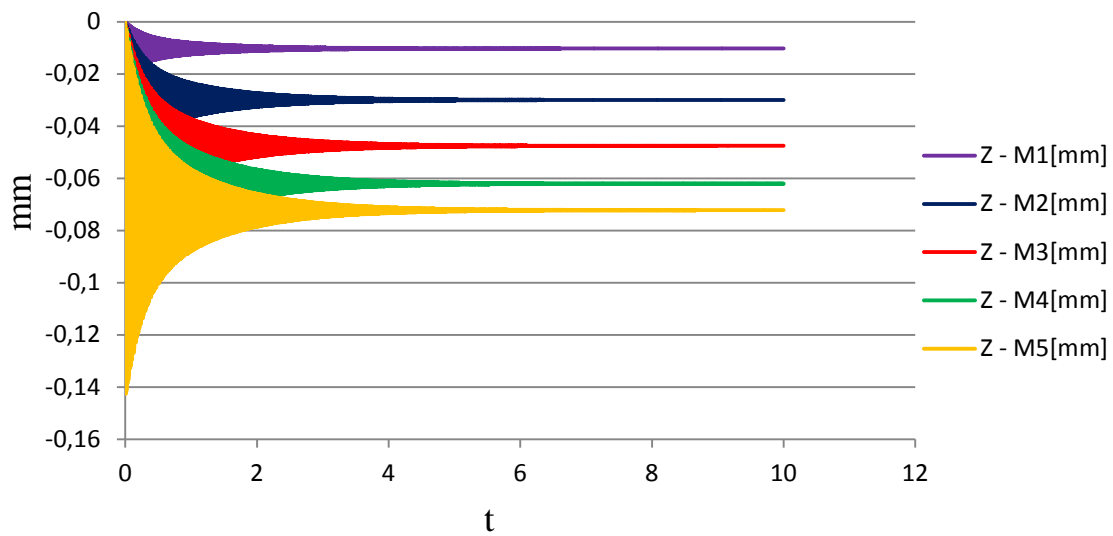


Figure 54: The deflection results for the elements from M1 to M5.

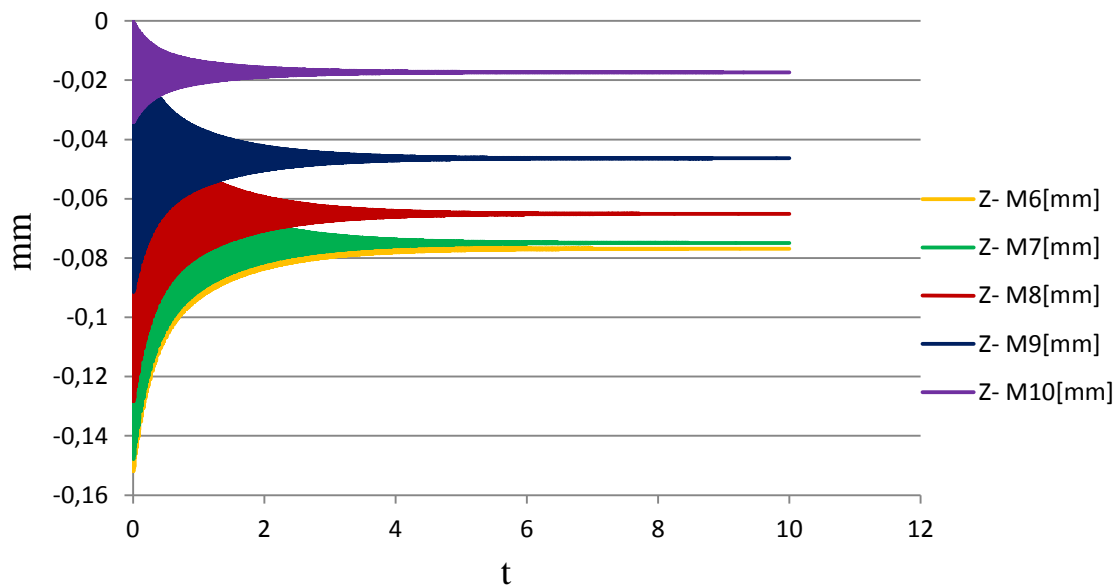


Figure 55: The deflection results for the element from M6 to M10.

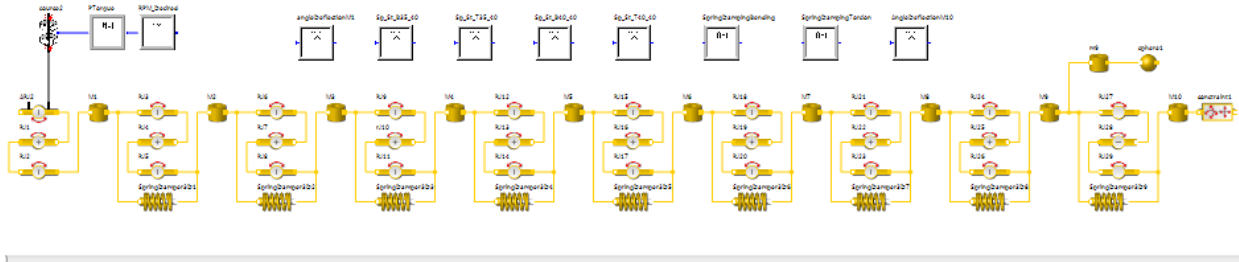


Figure 56: The setup of dynamic model due to kinematic analysis.

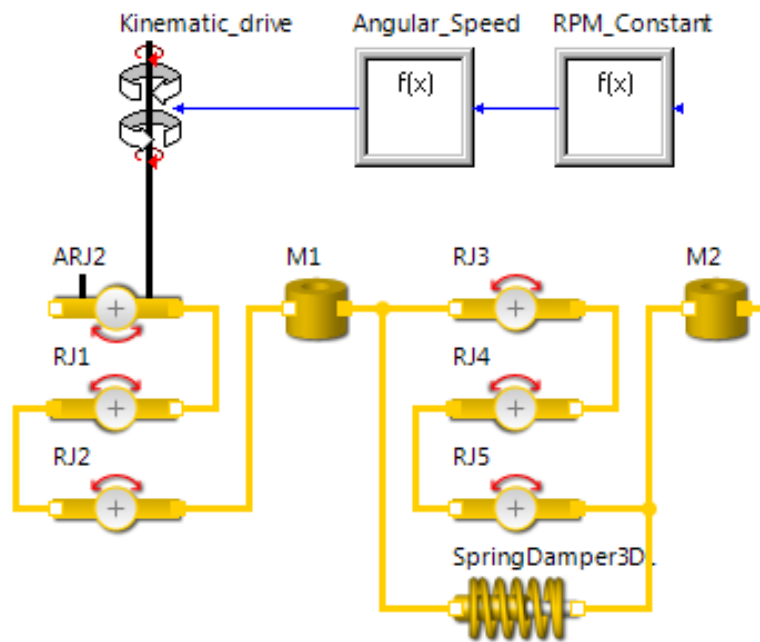


Figure 57: The connection of Kinematic drive and with 1st body element (M1).

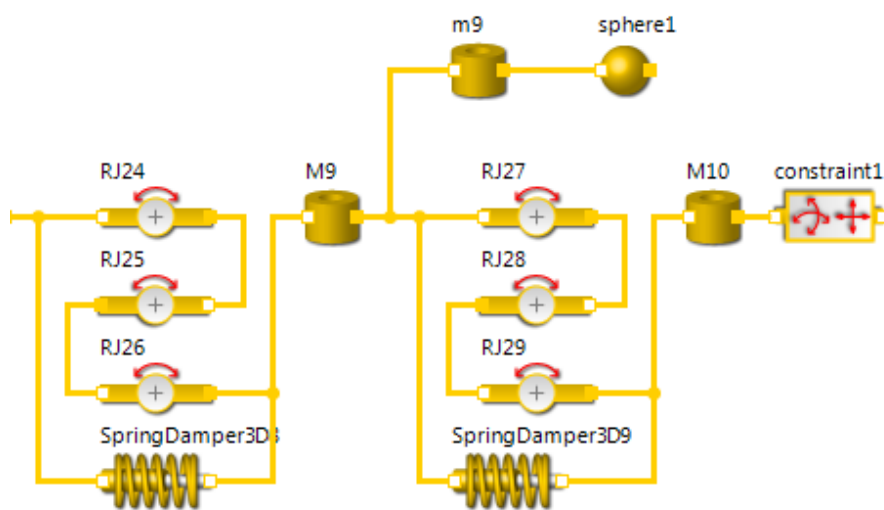


Figure 58: The connection of the constraint with the 10th body element (M10) and the radial load (sphere1).